The effect of 17-β estradiol therapy on bone mineral density and structure of alveolar bone in the ovariectomized rat model of postmenopausal osteoporosis

Bryan D. Johnston, BSc

Submitted in partial fulfillment of the requirements for the degree
Master of Science in Applied Health Sciences
(Health Sciences)

Supervisor: Wendy E. Ward, PhD

Faculty of Applied Health Sciences
Brock University
St. Catharines, ON.

Abstract

The ovariectomized (OVX) rat, a preclinical model for studying postmenopausal bone loss, may also be used to study differences in alveolar bone (AB). The objectives of this study were to quantify the differences in AB following estrogen replacement therapy (ERT), and to investigate the relationship between AB structure and density, and trabecular bone at the femoral neck (FN) and third lumbar vertebral body (LB3). Estrogen treated rats had a higher bone volume fraction (BV/TV) at the AB region (9.8% $P < 0.0001$), FN (12% $P < 0.0001$), and LB3 (11.5% $P < 0.0001$) compared to the OVX group. BV/TV of the AB was positively correlated with the BV/TV at the FN ($r = 0.69$ $P < 0.0001$) and the LB3 ($r = 0.75$ $P < 0.0001$). The trabecular number (Tb.N), trabecular separation (Tb.Sp), and structure model index (SMI) were also positively correlated ($P < 0.05$) between the AB and FN ($r = 0.42$, 0.49, and 0.73, respectfully) and between the AB and LB3 ($r = 0.44$, 0.63, and 0.69, respectfully). Given the capacity of AB to respond to ERT, future preclinical drug/nutritional intervention studies aimed at improving skeletal health should include the AB as a region of interest (ROI).

Key words: alveolar, bone, estrogen, ovariectomized, μ-CT

Acknowledgements

I would like to thank Dr. Wendy Ward for her guidance and support during this endeavor. I would also like to extend thanks to my committee members Dr. Peter Fritz and Dr. Sandra Sacco for their dedication and thoughtful comments.

I also thank Amanda Longo for performing body composition analyses and sharing the required tissues for my thesis research. Funding for this research was provided through a NSERC Discovery Grant and the micro-computed tomography system was funded through the Canada Foundation for Innovation.

Table of Contents

List of Figures

List of Tables

List of Abbreviations

AB	Alveolar bone
BMC	Bone mineral content
BMD	Bone mineral density
BMI	Body mass index
BV	Bone volume
BV/TV	Bone volume fraction
Ca	Calcium
CEJ	Cemento-enamel-junction
Conn.D	Connective density
Ct.BMD	Cortical bone mineral density
Ct.Th	Cortical thickness
CV	Coefficient of variation
DEXA	Dual-energy x-ray absorptiometry
E2	17-β estradiol
ERT	Estrogen replacement therapy
FDA	Food and Drug Administration
FN	Femoral neck
HEI	Healthy Eating Index
HRT	Hormone replacement therapy
LB3	Third lumbar vertebrae
M1	First molar
OPG	Osteoprotegrin

OVX	Ovariectomy
PBS	Phosphate buffered saline
PTH	Parathyroid hormone
pQCT	Peripheral quantitative computed tomography
RANKL	Receptor activator of nf kappa B ligand
ROI	Region of interest
SMI	Structure model index
Tb.BMD	Trabecular bone mineral density
Tb.N	Trabecular number
Tb.Pf	Trabecular pattern factor
Tb.Sp	Trabecular separation
Tb.Th	Trabecular thickness
TMD	Tissue mineral density
TRAP	Tartrate-resistant acid phosphatase
3D	Three dimensional
µ-CT	Micro-computed tomography

CHAPTER 1: LITERATURE REVIEW

1.1 Osteoporosis

A decline in ovarian production of estrogens at menopause often results in a rapid loss of trabecular microarchitecture, increased endocortical bone resorption, and increased cortical porosity; all culminating in the development of osteoporosis and the associated increased risk for fragility fracture (Figure 1) [1]. Specifically, the number and activity of osteoclasts increases to a point where the rate of bone resorption exceeds the rate of bone formation [2].

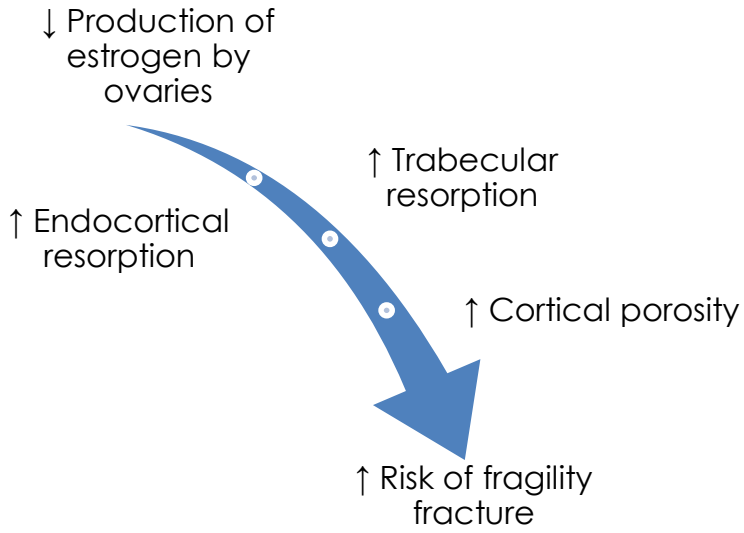

Figure 1: Overview of how osteoporosis develops after menopause
With the loss of endogenous estrogen production by the ovaries there is an increase in trabecular bone resorption, endocortical bone resorption and cortical porosity that elevates a woman's risk of experiencing a fragility fracture.

Based on data from the WHO Global Burden of Disease project in 2000, an estimated 56 million people around the world experience disability caused by a fracture [3]. In 2010, there were 2.32 million new hip fractures in adults over 50 years of age worldwide, and approximately half of those hip fractures were due to osteoporosis in the FN [4]. Based on osteoporosis prevalence rates reported in the

2010 US Census and NHANES (2005-2010), it is estimated that 10.2 million Americans over the age of 50 have osteoporosis while an additional 43.4 million having low bone mass that predisposes them to the development of osteoporosis [5]. In Canada, it is estimated that 1 in 5 women and 1 in 10 men will experience a hip fracture during their life. Even when adjusting for annual trends in mortality and hip fracture, the estimated lifetime risk of hip fracture remains high at 8.9% for women and 6.7% for men [6]. With the average hip fracture hospitalization in Canada costing approximately $20,000, the financial burden of osteoporosis over the 2007-2008 fiscal year was estimated at $2.3 billion dollars, or 1.3% of the entire Canadian healthcare budget [7]. It is well documented that women are disproportionally affected by osteoporosis compared to men, primarily due to the more sudden decline in estrogen production experienced at menopause whereas sex steroid levels decline more gradually in men [3-5, 8]. In the majority of postmenopausal women, the risk of experiencing a fragility fracture exceeds the risk of developing invasive breast cancer, stroke, and cardiovascular disease combined [9]. Moreover, there is substantive morbidity [10] associated with a fragility fracture and an increased risk of death; especially within the first year post-fracture [11]

1.1.1 Osteoporosis, estrogen and tooth loss

Osteoporosis not only increases a woman's risk of fragility fracture at the hip, spine and wrist, but is also associated with the loss of AB and teeth. [12-15]. For example, osteoporosis at the lumbar vertebrae, FN, or total hip is a significant predictor of molar tooth loss [12]. A 5-year longitudinal study of 404 postmenopausal women confirmed that women in the highest tertile of annual bone mineral density

(BMD) loss at the lumbar spine and FN had an adjusted relative risk of 1.38 and 1.27 for tooth loss, respectively, compared to women in the lowest tertile of annual BMD loss. [13]. In a longitudinal study of even greater duration, 7 years, the relative risk of tooth loss in 180 postmenopausal women (serum 17-β estradiol (E2) < 25 pg/ml) was 4.38 with each 1% annual decrease in whole body BMD [14]. A greater loss of AB height, and less alveolar crestal and subcrestal BMD – all critical for providing support for teeth – were also reported in a 2-year longitudinal study of 38 women with osteopenia and osteoporosis at the lumbar spine. Between the first and second molars in particular, estrogen-deficient (mean serum E2 < 30 pg/ml) women lost more alveolar crestal bone density compared to estrogen-sufficient (mean serum E2 > 40 pg/ml) women [15]. Because tooth retention [16, 17] and functional dentition [18, 19] are key determinants of nutritional status the maintenance of AB is important for overall health. Risk of many chronic diseases such as obesity, type 2 diabetes, cardiovascular disease and some cancers is elevated by poor diet. Thus, strategies that preserve the skeleton at key sites of fragility fracture – hip, spine, wrist – as well as AB in the jaw are important for healthy aging.

While ERT has been consistently shown to reduce fragility fractures at the hip, spine and wrist [20, 21] the effect on tooth retention and preserving AB has been less studied. However, a study of 42,171 postmenopausal women (aged ≤ 69 years) over a 2-year period as part of the Nurses' Health Study cohort, reported that current use of hormone replacement therapy (HRT; estrogen alone, in combination with progestin, or progestin alone) was associated with a 24% decrease in the risk of tooth loss. In women using conjugated estrogen alone, at a dose of 0.3 mg per day, the risk

of tooth loss was 31% lower compared to non-users [22]. In a cohort of 3,921 older women, median age of 81 years, current ERT (with or without progesterone) was associated with a 27% lower risk of tooth loss [23]. Another study showed that a group of postmenopausal women (72-95 years of age) who used ERT (reported as any use of estrogen) for greater than 8 years retained an average of 3.6 more teeth than women who never used ERT [24]. The duration of ERT (estrogen alone or in combination with progestogen) was also a significant predictor of total and posterior teeth remaining in a group of 330 postmenopausal Japanese women [25]. The mechanism behind tooth retention and ERT remains unclear, but one 3-year longitudinal study of 135 women aged 41-70 years concluded that women receiving 0.625 mg conjugated equine estrogen with or without 2.5 mg medroxyprogesterone acetate experienced a 0.9% increase in AB mass, as assessed by digitized radiographs, compared to non-users [26]. HRT or ERT may therefore work to increase the stability of the tooth-supporting AB and thereby promote tooth retention and the opportunity to consume a greater variety of foods.

1.1.2 Tooth loss and nutritional status

Retention of natural teeth is associated with healthier nutrient intakes that may have a role in prevention of chronic disease. For example, dietary calcium (Ca) has been studied in relation to tooth loss because achieving recommended intakes of dietary Ca, in particular, is important for attenuating bone loss after menopause and during aging. As such, the recommended intake of Ca is 1200 mg per day in women aged 51-70 years and men over age 70 years [27]. Among older men and women (≥ 65 years of age) with unknown smoking status, higher daily intake of Ca (884 versus

805 mg Ca) was associated with a greater number of teeth (≥ 21 versus 11-20 teeth) [16]. Another study reported lower tooth loss in a placebo-controlled 2-year study of non-smoking women taking a Ca supplement of 500 mg per day; smoking women were excluded because smoking is a risk factor for tooth loss [14].

Fruit and vegetable intake in relation to tooth loss has also been studied. Data from NHANES III, a large cross-sectional study of Americans over age 50, showed a reduced number of posterior teeth associated with a lower daily intake of the recommended amount of fruit servings as reflected in a lower Healthy Eating Index (HEI) score and a higher body mass index (BMI) [18]. Additionally, having no posterior teeth was associated with a lower daily intake of the recommended amount of vegetable servings, also reflected in a lower HEI score [18]. Even when controlling for socio-economic status, inadequate dentition (defined by < 21 teeth remaining) was associated with reduced intakes of fruit (stone fruits and grapes/berries) and vegetable (stir-fried or mixed vegetables, sweetcorn/corn on the cob, mushrooms, lettuce, and soy beans/tofu) in a sample of 530 dentate Australian men and women over the age of 55 [19]. The link between tooth loss and reduced fruit and vegetable intake is important since a recent comprehensive review concluded that fruit and vegetable consumption was associated with a reduced risk of chronic diseases such as hypertension, coronary heart disease, and stroke [28]. Interestingly the relationship between a lower BMD in postmenopausal osteoporosis, higher rates of tooth loss, and lower fruit and vegetable intake comes full circle given the study of 670 postmenopausal Chinese women that found higher fruit and vegetable intake was associated with greater whole body, lumbar spine, and hip BMD. The regression

model predicted that a daily increase of 100 g of fruits and vegetables was associated with a 6, 10, and 6 mg/cm^2 greater BMD at the whole body, lumbar spine, and hip, respectively. [29].

The relationship between osteoporosis, tooth loss, and compromised nutrition may prove to be cyclical (Figure 2) since compromised nutrition could exacerbate osteoporosis. As discussed in section 1.1.1, HRT or ERT has been shown to promote tooth retention and may intervene in this self-perpetuating, negative cycle of tooth loss and the consequent greater risk of chronic disease development. Moreover, there are other pharmacological agents or diet interventions that may prove useful in stopping the cycle shown in Figure 2. The ovariectomized rat can be used to evaluate the effectiveness of an intervention for preserving AB [30, 31]. Findings from these studies provide an important step in developing interventions to promote and support bone health – including the retention of natural teeth – for postmenopausal women.

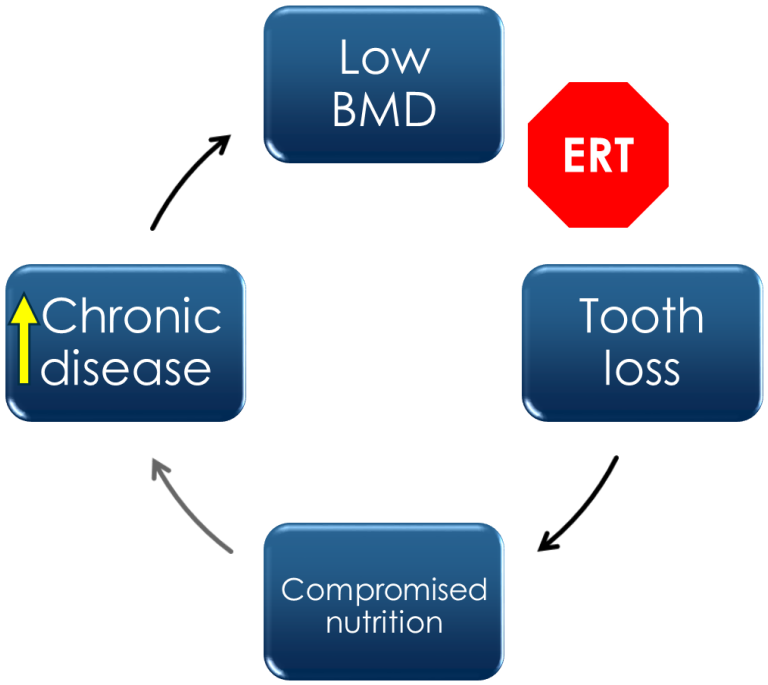

Figure 2: **Cyclical relationship among low BMD, tooth loss, compromised nutrition and risk for chronic disease**
ERT/HRT or other interventions that benefit other skeletal sites such as hip, spine and wrist may also prevent or slow the progression from low BMD to tooth loss. Retention of natural teeth allows individuals to eat a more healthful diet that is associated with a reduced risk of chronic disease.

1.2. The ovariectomized rat model

The OVX rat model is an approved preclinical model by the Food and Drug Administration (FDA) [32] for studying how the decline in endogenous estrogen production by the ovaries at menopause leads to postmenopausal osteoporosis, and how potential interventions can preserve bone metabolism in this state. Although the FDA guidelines do not specify which strain of rat to use, it is important to be aware that there can be differences in BMD, bone size, and biomechanical bone strength among inbred rat strains [33]. Interventions include pharmacological agents as well as lifestyle strategies such as diet. By 12 weeks of age, the female Sprague-Dawley rat – among the most common strains studied – has reached sexual maturity and has

achieved peak bone mass for the whole body, femora, and tibiae [34]. Peak bone mass was defined as the point at which the rat skeleton had accrued its greatest amount of areal BMD determined by dual-energy x-ray absorptiometry (DEXA) at the whole body, femur, and tibia. However, longitudinal bone growth continues in the female rat until the epiphyseal growth plates close. At 12 weeks of age, the distal tibia growth plate has closed while the proximal tibia, and lumbar vertebral growth plates remain open until 15, and 21 months respectively [35]. Despite the continued skeletal growth, rats are commonly ovariectomized at 12 weeks of age since the rats are sexually mature and therefore capable of modeling bone loss due to estrogen deficiency [36]. By 9 months of age, longitudinal bone growth at the proximal tibia metaphysis has slowed to 3 μm/day, while growth at the lumbar vertebral body has slowed to < 1 μm/day [37].

Two developmental stages have been used to describe the adult rat skeleton: 'mature' from 3-6 months of age and 'aged' ≥ 6 months of age. Skeletal growth is rapid from 1-3 months, reduced from 3-6 months and negligible past 6 months of age [38]. In addition to continued longitudinal bone growth, the extent of OVX-induced bone loss is dependent on both the skeletal site and the time since OVX. For example, in the proximal tibia, a significant decrease in trabecular bone volume (BV) is observed 2 weeks post-OVX compared to sham control with a plateau by 14 weeks post-OVX [39]. At the FN, a significant decrease in trabecular BV occurred at 4 weeks post-OVX with a plateau by 39 weeks post-OVX [40]. The lumbar vertebrae was much more resistant to OVX-induced changes in trabecular BV than either the

proximal tibia or FN. It was not until 7 weeks post-OVX that a decrease in trabecular BV was significant and reached a plateau between 39 and 77 weeks post-OVX [41].

The effect of time since OVX on the rat mandible is less clear so the studies discussed in this review are subsequently divided into those that are ≤ 12 weeks in duration and those that are ≥ 12 weeks duration after OVX. This time point was chosen since a 12-week period after OVX has been shown to be sufficient to decrease trabecular BV at the proximal tibia [39], FN [40], and lumbar vertebrae [41]. Figure 3 is an image of a hemimandible from a Sprague-Dawley rat with key landmarks and directions highlighted and serves as a guide to the specific study regions of interest (ROI) discussed in the next section. Similarly, Figures 4 through 6 are included to assist the reader in identifying regions that have been analyzed in the studies that are discussed in this review. Figure 4 is a sagittal slice through the first molar (M1) with the interradicular septum containing AB highlighted. Figure 5 is a three-dimensional (3D) rendering of the 4 roots of M1 (mesial, lingual, buccal, and distal roots) and shows how these roots enclose the AB of the interradicular septum. Figure 6 is a 3D rendering of M1 in its bony socket and viewed as a cut-away to show landmarks used to define AB ROI.

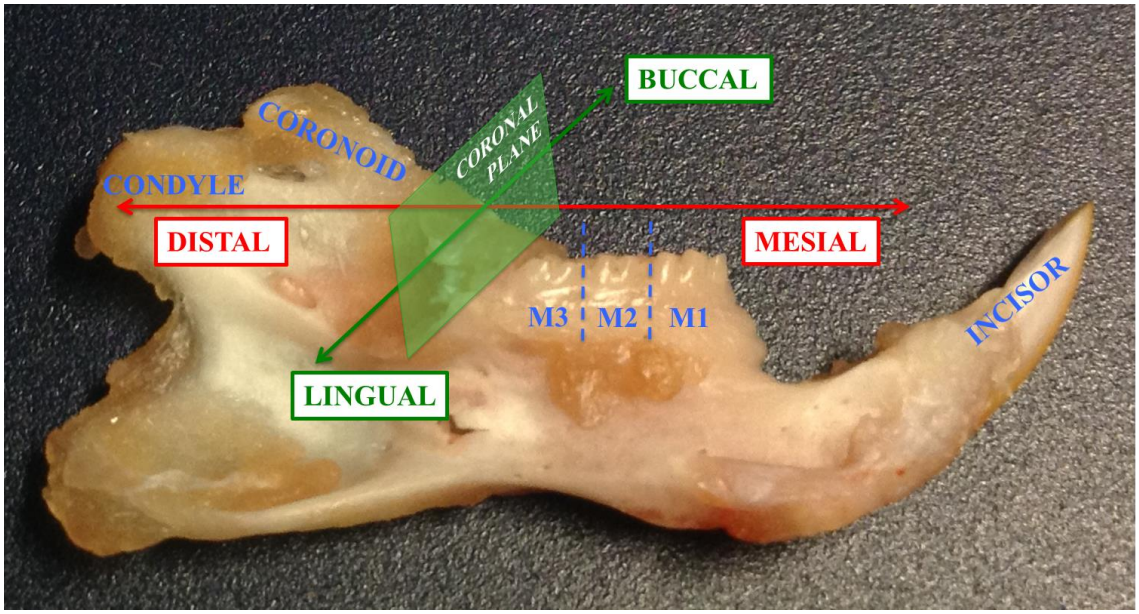

Figure 3: **Hemimandible from a 6-month old Sprague-Dawley rat**
From right to left: incisor, 1st molar (M1), 2nd molar (M2), 3rd molar (M3), the coronoid process and condyle. Mesial is the front, distal the back, buccal the lateral side, lingual the medial side and the coronal plane divides the mandible into mesial and distal portions.

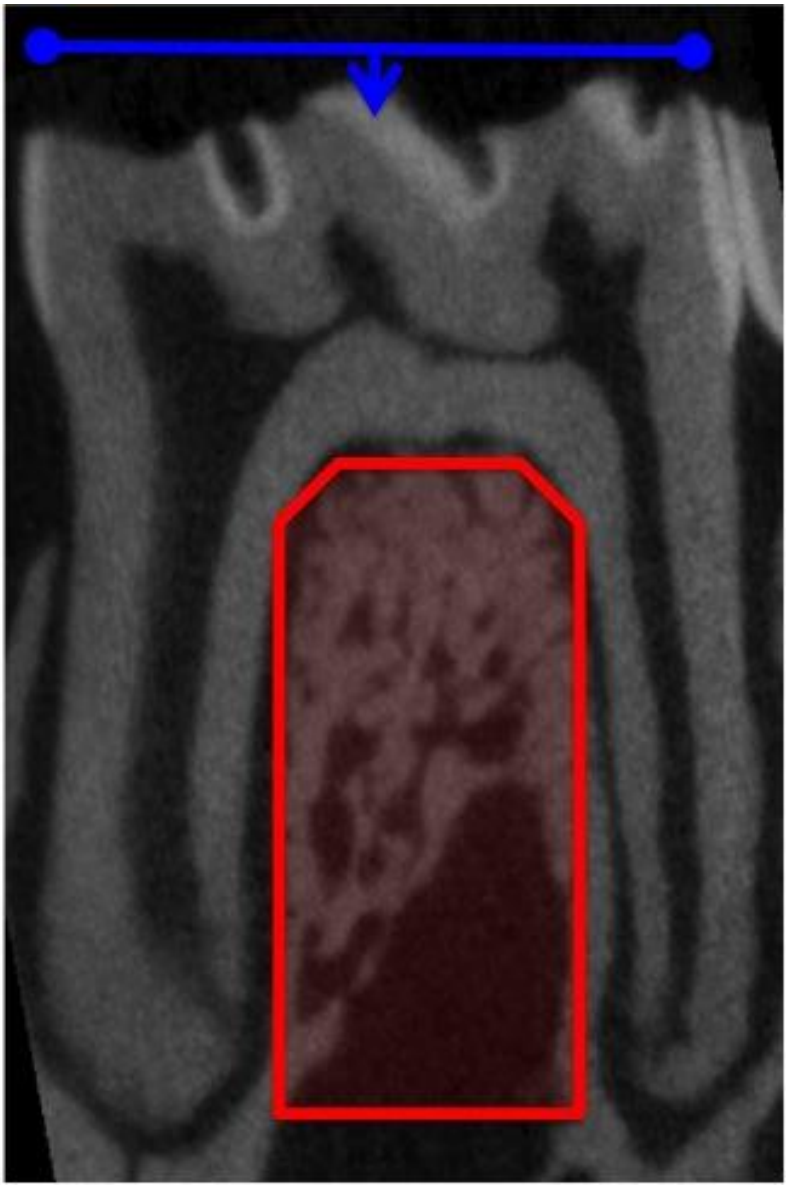

Figure 4: Sagittal slice through molar 1 (M1) of a 6 month old Sprague-Dawley rat with interradicular septum
The interradicular septum is highlighted in red and extends from the furcation roof to the root apices. The occlusal surface of M1 is highlighted in blue and the arrowhead denotes the approximate location of the central sulcus.

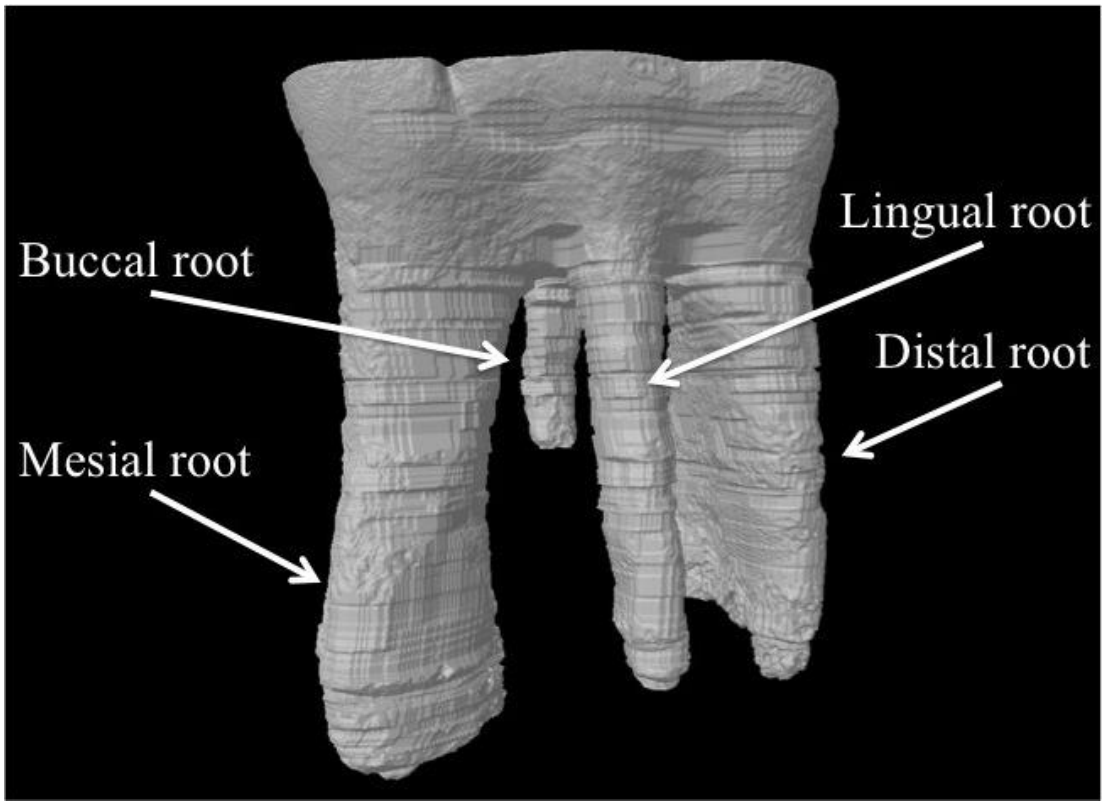

Figure 5: Four roots of M1
The mesial, distal, buccal, and lingual roots enclose the AB of the interradicular septum.

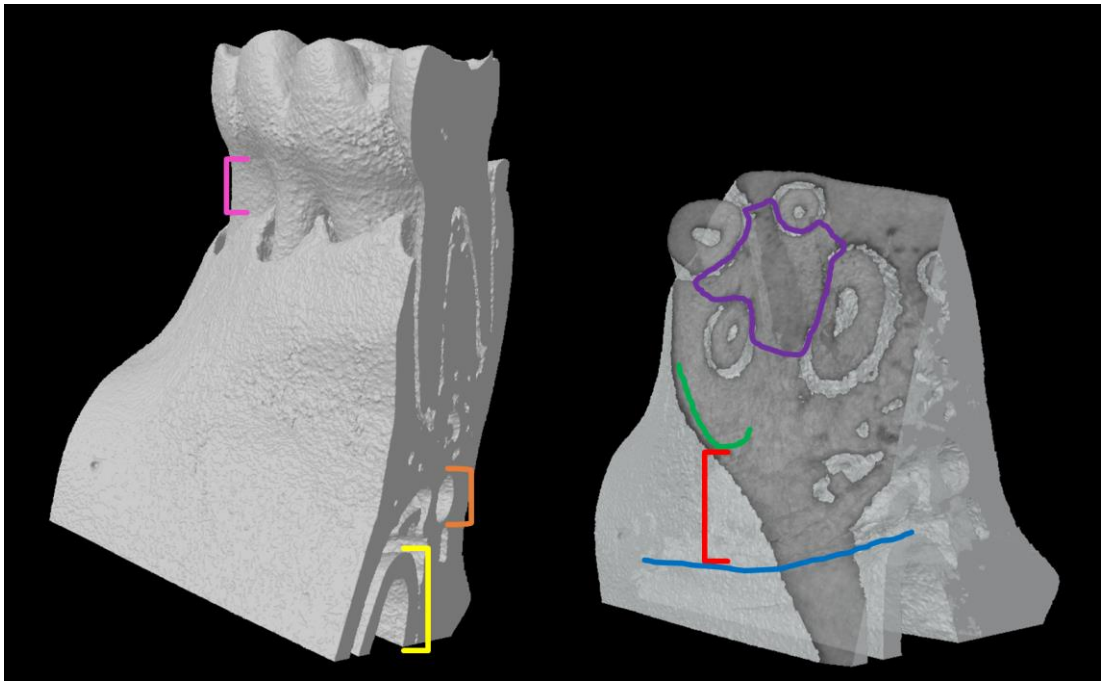

Figure 6: Landmarks to define ROI of AB at M1
M1 in its bony socket (left) with the distance between the cemento-enamel junction (CEJ) and bone crest (pink), the mandibular canal (orange), and the incisor root (yellow). In a cut-away model of M1 in its bony socket (right) the AB of the interradicular septum (purple) is superior to the AB (red) between the incisor crest (blue) and mesial root apex (green).

1.2.1 Short-term effects of OVX on mandibular bone: findings from studies less than 12 weeks after OVX

In only three of the six studies with an OVX duration < 12 weeks, OVX reduced either AB structure [42, 43] or density [44] (Table 1). In those studies, the time since OVX was approximately nine weeks and the rats were ovariectomized at 17, 25 and 26 weeks of age [42-44]. The first study [42] used histomorphometry to measure the M1 sagittal surface containing the central sulcus of the occlusal surface and both the mesial and distal root canals. The ROI was the entire interradicular septum of M1 extending from the furcation roof to the mesial and distal root apices (Figure 4). Relative to the sham group, there was lower BV and Tb.N with higher Tb.Sp but no difference in trabecular thickness (Tb.Th) between the sham and OVX group.

Similar results were reported by a study that also investigated AB nine weeks after OVX, the only difference being an older age at OVX, 25 versus 17 weeks [43]. The hemimandibles were scanned via micro-computed tomography (μ-CT) between the mesial and distal roots of M1 at a resolution of 50 μm. The ROI was delineated inferiorly by a plane connecting the apices of the buccal and lingual roots (Figure 5), and superiorly by a contour along the interradicular septum (Figure 4). Relative to the sham group, there was less BV and Tb.Th with greater Tb.Sp. There was no difference in Tb.N between the sham and OVX group.

Changes in the AB density of Sprague-Dawley rats ovariectomized at 26 weeks of age and maintained for the same nine weeks post-OVX were also reported [44]. To measure the tissue mineral density (TMD) distribution, hemimandibles were cut into 5 mm sections and scanned via μ-CT at a resolution of 20 μm. The ROI was a

volume of AB extending 200 μm from the surface of each tooth along the 5 mm section; if visualized in 3D the ROI would be a 200 μm thick cast of the tooth surfaces in direct contact with the AB. This ROI included both the periodontal ligament (~ 150 μm) and the AB in direct contact with the tooth surface (~ 50 μm). There were higher standardized grey values of the TMD distribution at the 5^{th} percentile in the OVX group compared to the sham group. Higher grey values at the 5^{th} percentile implied more immature bone formation due to accelerated bone remodeling. There was also a higher standardized TMD distribution coefficient of variation (CV) in the OVX group compared to the sham group. A greater CV suggested that bone turnover increased. In summary, these studies have shown that by nine weeks post-OVX there is a reduced AB volume and increased Tb.Sp [42, 43] and the stability of the AB directly supporting the molars is also compromised [44].

Of the studies with an OVX duration < 12 weeks, that did not report an effect on AB, two had times post-OVX of less than nine weeks [45, 46] and one had a time post-OVX of exactly nine weeks [47]. Different techniques used to measure changes to AB may also explain why, among the studies with an OVX duration of approximately 9 weeks, one study reported no effects [47] while three others reported effects [42-44]. The study with the shortest study period post-OVX measured mandibular BMD in Sprague-Dawley rats ovariectomized at four weeks of age and x-ray radiographs of hemimandibles were taken four weeks after OVX [45]. The ROI began 1.5 cm mesial to M1 and extended until the end of the AB supporting the distal root of M3 (Figure 3). The ROI was delineated inferiorly by the crest of the incisor root and superiorly by the contours of the molar roots (Figure 6). This ROI included

the AB supporting M1-M3 and the surrounding cortical bone. There was no difference in BMD between the sham and OVX group. AB loss was also measured by calculating the difference in height between the CEJ and the bone crest at the midpoint of the mesial root (Figure 6) of each molar. There was no difference in AB loss between the sham and OVX group.

At five weeks post-OVX, the mandibular BMD of Sprague-Dawley rats ovariectomized at 13 weeks was measured using DEXA [46]. The ROI of left hemimandibles was a rectangle extending from the angle mesial to M1 until the distal root of M3 (Figure 3). The following were included in the ROI: molars, AB, cortical bone, and the incisor root. There was no difference in BMD between the sham and OVX group. Additionally, the mandibular bone area fraction and area moment of inertia were measured using coronal sections (Figure 3) of the distal most aspect of the M1 mesial root (Figure 5). An image of the newly exposed surface constituted the ROI and included the AB, cortical bone, and incisor root. There was no difference in bone area fraction or area moment of inertia between the sham and OVX group.

Even nine weeks after OVX, Wistar rats ovariectomized at 17 weeks of age showed no difference in the mandibular BMD between the sham and OVX group [47]. The mandibular BMD was measured by DEXA equipped with small animal software. The ROI was a rectangle encompassing the alveolar, condylar, and coronoid processes (Figure 3); the molar crowns and incisor were removed. Since changes in AB structure [42, 43] and density [44] have been reported by ~ nine weeks post-OVX, it is possible that DEXA may not be sensitive enough to detect the OVX-induced changes in the rat mandible. Studies that follow for a longer time period after

OVX are likely needed to detect OVX-induced loss of mandibular BMD by DEXA. Future studies that use μ-CT to measure changes in AB structure in response to OVX are also needed. It is likely that μ-CT would detect a more subtle change in AB after a shorter amount of time post-OVX than DEXA due to its superior resolution, ability to quantify structural changes, and highly specific ROI in 3D. Also, in order to detect a robust change in AB after OVX that can be correlated with changes at other typical skeletal sites such as the long bones and lumbar vertebrae, a time post-OVX of greater than 12 weeks is likely needed.

Table 1: Summary of studies investigating changes in mandibular health in rats less than 12 weeks after OVX

Rat strain	Sample size per group	Age at OVX (wks)	Time post-OVX (wks)	Diet	Technology	Main findings for mandible, compared to sham control	Reference
Sprague-Dawley	*n* = 5	4	4	0.89 % Ca	Radiographs	•No change in BMD •No AB loss	[45]
Sprague-Dawley	*n* = 8	13	5	1.00 % Ca	DEXA, Histomorphometry Stereology	•No change in BMD, bone area fraction, or area moment of inertia	[46]
Fischer	*n* = 8	17	9	Unknown	Histomorphometry	•25 % decrease in BV/TV •17 % decrease in Tb.N •32 % increase in Tb.Sp •No change in Tb.Th	[42]
Sprague-Dawley	*n* = 10	26	9	Unknown	µ-CT	•7 % increase in the TMD distribution grey values at the 5^{th} percentile •25 % increase in the TMD distribution CV	[44]
Wistar	*n* = 6	17	9	Unknown	DEXA	•No change in BMD	[47]
Wistar	*n* = 6	25	9	1.17 % Ca, 0.91 % P	µ-CT	•15 % decrease in BV/TV •14 % decrease in Tb.Th •22 % increase in Tb.Sp •No change in Tb.N	[43]

AB, alveolar bone; BMD, bone mineral density; BV/TV, bone volume fraction; DEXA, dual-energy x-ray absorptiometry; Tb.N, trabecular number; Tb.Sp, trabecular separation; Tb.Th, trabecular thickness; TMD, tissue mineral density; µ-CT, micro-computed tomography

1.2.2 Longer-term effects of OVX on mandibular bone: findings from studies that are 12 weeks or longer after OVX

All of the studies with an OVX duration of longer than 12 weeks (Table 2) report a reduction in bone mineral and/or structural changes in AB. Of these nine studies, five reported changes in AB structure [48-52], three reported significant reductions in the BMD of AB [53-55] and a single study reported a decrease in the Ct.Th of AB [56].

Two studies used conventional histomorphometric methods to report changes in AB structure following OVX [48, 51]. One study ovariectomized rats at six weeks of age and studied them until 12 weeks post-OVX [48]. To measure the mandibular histomorphometry, hemimandibles were sectioned coronally (Figure 3) into 50 μm thick slices. The ROI was a rectangle, with an area of 0.135 mm^2, inferior to the apices of the buccal and lingual roots of M1 (Figure 5) and superior to the mandibular canal (Figure 6). There was a decrease in BV between the sham group and OVX group. Another study ovariectomized Sprague-Dawley rats at 26 weeks and maintained them for 29 weeks [51]. To measure the mandibular bone area fraction and the area moment of inertia, the left hemimandibles were sectioned coronally (Figure 3) between the mesial and buccal roots of M1 (Figure 5) and also between the roots of M2. The ROI for the bone area fraction was the entire surface of the M1 section with the molar crown/roots and incisor removed. The ROI for the area moment of inertia was the entire surface of the M2 section with the incisor removed. The bone area fraction of the OVX group was less than the sham group. There was no difference in the moment of inertia between sham and OVX groups.

The remaining three studies to report changes in AB structure used μ-CT [49, 50, 52]. To measure the mandibular morphometry of rats ovariectomized at 11 weeks and maintained for 16 weeks, left hemimandibles were scanned via μ-CT beginning at the mesial plane of M1 and extending 25 slices toward the distal root (Figure 5); the scan was at a resolution of 15 μm [49].

The ROI was delineated superiorly by the apex of the M1 mesial root (Figure 5) and inferiorly by the crest of the incisor socket (Figure 6). The buccal and lingual walls of cortical bone that flanked the ROI were removed. Relative to the sham group, there was a lower BV, lower Tb.Th, higher Tb.Sp and a higher SMI in the OVX group. A higher SMI indicated a shift in trabeculae shape from plate-like to rod-like; rod-like trabeculae are thinner trabeculae and are thus indicative of structurally-compromised AB.

Another study measured the mandibular morphometry of rats ovariectomized at 28 weeks and studied 17 weeks later by scanning the left hemimandibles using μ-CT. This analysis was done between the mesial and distal borders of M1 (Figure 5) at a resolution of 16 μm [50]. The ROI was an interpolated shape encompassing the AB from the apices of the buccal and lingual roots (Figure 5) to the crest of the incisor (Figure 6), and from the mesial to distal surfaces of the M1 interradicular septum (Figure 5). Relative to the sham group, there was a lower Tb.N and connectivity density in the OVX group but no differences in BV or Tb.Th between the sham and OVX group.

To investigate longer-term changes in mandibular morphometry, the right hemimandibles of rats ovariectomized at 26 weeks and studied 52 weeks later were scanned using μ-CT at a resolution of 20 μm [52]. The ROI was the interradicular septum of M1 delineated inferiorly by a straight line between the mesial and distal roots (Figure 4). Only a single sagittal slice exposing the interradicular septum of M1 was used for the ROI, not the entire volume of the interradicular septum. Relative to the sham group there was a lower BV, a lower Tb.Th, a lower Tb.N, and a higher Tb.Sp in the OVX group – indicating compromised structure of AB.

Of the studies to evaluate changes in mandibular BMD following OVX using DEXA [50, 51, 55], none reported any changes in BMD while each of the studies reported changes in

mandibular density or structure by either peripheral quantitative computed tomography (pQCT) [55], μ-CT [50] or histomorphometry [51]. Of the three studies to evaluate changes in mandibular density by pQCT, all three reported a loss of BMD post-OVX [53-55]. These studies provide evidence that mandibular BMD measured by DEXA cannot represent the changes in AB following OVX in the rat and that higher resolution techniques such as pQCT or μ-CT are needed.

In a study of rats ovariectomized at 35 weeks and studied at 13 weeks after OVX, the BMD of hemimandibles was measured via pQCT between the mesial root of M1 and the distal root of M2 (Figure 3) at a voxel size of 100 μm and a section thickness of 750 μm [53]. The ROI was the entire surface of each coronal section with the molar crowns, roots and the incisor root removed; this included both trabecular and cortical bone. Relative to the sham group, there was a lower total, trabecular and cortical bone mineral density (Ct.BMD) in the OVX group.

Another study in younger ovariectomized rats (13 weeks old) that were studied 16 weeks post-OVX, scanned hemimandibles using pQCT from the mesial border of M1 to the distal border of M3 (Figure 3) [55]. The ROI was the surface of each coronal pQCT section with the molar crowns/roots and the incisor root removed. The lowest trabecular BMD (Tb.BMD) in the OVX group compared to the sham group was observed 3.5 mm from the mesial border of M1. There was no difference between the sham group and the OVX group Ct.BMD. Additionally, the hemimandibles of rats ovariectomized at 26 weeks and maintained for 16 weeks post-OVX were scanned via pQCT at one 750 μm thick coronal slice through the midpoint of M1 (Figure 3) at an in-plane resolution of 100 μm [54]. The ROI was the entire surface of the coronal slice with the molar crown/roots and the incisor root removed. There was a lower total mandibular BMD in the OVX group compared to the sham group.

A long-term study of rats ovariectomized at 13 weeks and maintained for 52 weeks post-OVX measured changes in mandibular cortical bone thickness [56]. Left hemimandibles were exposed to a 70 kV, 7 mA x-ray source and images were digitally captured at a resolution of 12.5 line pairs/mm with a total image size of 640 by 480 pixels. The ROI was a computer-generated contoured shape encompassing the lower mandibular border; it began superiorly where the lower border met the incisor root and extended to the most inferior aspect of the lower border. There was a lower mandibular Ct.Th in the OVX group compared to the sham group.

In summary, the longer the time since OVX, the greater the magnitude of the observed changes in AB structure. Likewise the age of the rat at OVX determines its skeletal maturity, and thus changes in bone density and structure in a mature rat (> 3 months of age) skeleton is more likely to mimic those in a mature adult human skeleton. An immature rat (< 3 months of age) skeleton would experience competing skeletal growth after OVX and that may skew any OVX-induced changes. Robust changes to AB following OVX have consistently been reported in studies that analyze mandible outcomes at or after 12 weeks after OVX. The combination of studying a rat with a mature skeleton (at least 12 weeks of age (~ 3 months) and ideally closer to 6 months of age at OVX to exclude skeletal growth) and a time post-OVX of at least 12 weeks, would yield changes to AB structure and density that are optimal to represent postmenopausal bone loss. Future studies developing interventions to preserve AB should consider this time frame.

Table 2: Summary of studies investigating mandibular health in rats for 12 weeks or more after OVX

Rat strain	Sample size per group	Age at OVX (wks)	OVX duration (wks)	Diet	Technology	Main findings for mandible, compared to sham control	Reference
Wistar	*n* = 5	6	12	1.15 % Ca, 0.35 % P	Histomorphometry	•24 % decrease in BV	[48]
Wistar	*n* = 15	35	13	0.01 % Ca	pQCT	•7 % decrease in total BMD •11 % decrease in Tb.BMD •1 % decrease in Ct. BMD	[53]
Sprague-Dawley	*n* = 6	13	16	Unknown	DEXA, pQCT	•No change in BMD •13 % decrease in Tb.BMD •No change in Ct.BMD	[55]
Lewis-Brown-Norway	*n* = 12	11	16	Unknown	µ-CT	•18 % decrease in BV/TV •28 % decrease in Tb.Th •67 % increase in Tb.Sp •22 % increase in SMI	[49]
Wistar	*n* = 12	26	16	0.1 % Ca	pQCT	•3 % decrease in total BMD	[54]
Sprague-Dawley	*n* = 11	28	17	1.1 % Ca, 0.80 % P,	DEXA, µ-CT	•No change in BMD •6 % decrease in Tb.N •19 % decrease in Conn.D •No change in BV/TV •No change in Tb.Th	[50]
Sprague-Dawley	*n* = 15	26	29	1.0 % Ca	DEXA, Histomorphometry	•No change in total or molar region BMD •8 % decrease in bone area fraction	[51]

						•No change in area moment of inertia	
Lewis-Brown-Norway	*n* = 6	13	52	Unknown	Radiograph	•16 % decrease in Ct.Th	[56]
Fischer	*n* = 6	26	52	1.15 % Ca, 0.88 % P, 0.80 IU/g vit D^3	µ-CT	•75 % decrease in BV/TV •46 % decrease in Tb.Th •58 % decrease in Tb.N •354 % increase in Tb.Sp	[52]

BMD, bone mineral density; Tb.BMD, trabecular BMD; Ct.BMD, cortical BMD; BV, bone volume (2D); BV/TV, bone volume (3D); Tb.N, trabecular number; Tb.Sp, trabecular separation; Tb.Th, trabecular thickness; Ct.Th, cortical thickness; SMI, structure model index; Conn.D, connective density; DEXA, dual-energy x-ray absorptiometry; pQCT, peripheral quantitative computed tomography; µ-CT, micro-computed tomography

1.3 Effect of dietary calcium on mandibular health in ovariectomized rats

In addition to considering age at OVX and time from OVX, dietary Ca levels are also important to consider. Two studies [48, 52] used the same level of Ca in the diet (1.15 % Ca) but studied the rats for different periods of time post-OVX and reported different percent changes in AB volume (24% versus 75%). Thus, the observed differences in AB volume are due to differences in the time post-OVX. In other studies that were of similar length after OVX (16 weeks [54] versus 13 weeks [53]), different dietary Ca levels affected mandibular outcomes. For example, a tenfold difference in dietary Ca, of which both levels were considered 'low Ca' (0.1 % Ca and 0.01% Ca), resulted in a 2.88% and 7.35% decrease in total mandibular BMD, respectively. Thus, mandibular health is dependent on the age at OVX, time post-OVX and the level of dietary Ca. To control for such variation, future studies could use semi-purified diet such as the AIN93M that is specially formulated to meet the nutritional needs of the adult rat [57] and facilitates a standardization of the effects of diet on bone outcomes. Although not specifically studied in the ovariectomized rat model, other aspects of a diet including macronutrient or micronutrient content can also likely affect the outcomes of mandibular health if not tightly controlled among studies.

1.4 ERT therapy preserves mandibular health in ovariectomized rats

A single human trial has reported higher AB density with ERT [26], yet with the ovariectomized rat model it is clear that estrogen treatment can preserve both the periodontium [58, 59] and AB density [30, 60] and also reduce mandibular bone turnover [31] (Table 3). Rats that were ovariectomized at an unreported age and maintained for two weeks were divided into sham, OVX, and OVX + estrogen, and were implanted with mini osmotic pumps to continuously deliver either vehicle (sham and OVX groups) or estrogen (OVX + estrogen group) [58]. The

treatment that the OVX + estrogen group received was 1.5 μg/day of E2; this dose was not standardized to body weight so it is difficult to place in the context of the other studies. To measure mandibular osteoclastogenesis, right hemimandibles were sectioned into 5 μm thick slices at the M1 mesial root (Figure 5) and stained for tartrate-resistant acid phosphatase (TRAP) activity. The ROI was the buccal periodontium surrounding the mesial root of M1. At two weeks post-OVX, there were less nuclei/osteoclast observed in the OVX + estrogen group compared to the OVX group. There was no difference in the number of nuclei/osteoclast between the sham and OVX + estrogen groups. Thus, estrogen treatment attenuated the OVX-induced osteoclastogenesis observed in the rat buccal periodontium of M1.

Another study in rats that were ovariectomized at 13 weeks of age, were administered E2 by injection at a dose of 10 μg/kg for 5 days/week, for seven weeks post-OVX [59]. To measure the periodontal ligament space, left hemimandibles were cut sagittally at the buccal/lingual midpoint (Figure 5) to expose M1-M3, and were scanned via scanning electron microscopy. The ROI was the distance between a molar root surface and the supporting AB at three randomly chosen sites per rat. There was an increase in the periodontal ligament space between the sham and OVX groups. Estrogen treatment inhibited the expansion of the periodontal ligament space, and by extension, AB resorption.

Rats ovariectomized at 11 weeks received a daily subcutaneous injection of E2 at a dose of 20 μg/kg for 11 weeks [30]. To measure the AB density, hemimandibles were sectioned into 6 μm thick slices in the coronal plane (Figure 3) between the mesial and distal roots of M1 (Figure 5). The ROI was the volume of AB within 1000 μm of the furcation roof on five equally spaced slices within the M1 interradicular septum. There was a lower AB density in the OVX group

compared to the sham group. There was no difference in AB density between the sham and the OVX + estrogen group.

A similar study also used Wistar rats ovariectomized at 11 weeks, but treated the rats with an oral dose of estriol at 100 μg/kg, 5 days/week for 12 weeks post-OVX [60]. To measure changes in Tb.BMD and bone mineral content (BMC), the hemimandibles were scanned using pQCT at a resolution of 100 μm at 11 slices beginning 0.5 mm from the mesial boarder of M1 to the distal border of M3 (Figure 3). The ROI extended from the superior edge of the incisor root (Figure 6) to the molar furcation roof and excluded the molar crown, roots, and surrounding cortical bone. The OVX + estrogen treated group had a higher Tb.BMD and BMC at multiple slices compared to the OVX group; the sites of greatest AB preservation were the slices directly beneath M1 and M2.

To measure longer-term changes in mandibular bone remodeling rats were ovariectomized at 13 weeks and left untreated for 52 weeks post-OVX [31]. After the 52 week period, one group received estrogen treatment for 10 weeks as a subcutaneous injection of E2 for four days each week at a dose of 10 μg/kg. Flurochrome bone markers were also administered at 17 and seven days prior to necropsy. To measure the mandibular histomorphometry, right hemimandibles were sectioned coronally at M2 (Figure 3) into 30 μm thick slices and visualized with a fluorescence microscope to quantify bone turnover. There were two ROIs, the periosteal bone surface around the outside of the mandibular cortical bone, and the endosteal bone surface around the trabeculae within the M2 supporting AB. On the periosteal surface, the mineralizing surface of the OVX group was higher than the OVX + estrogen group. On the endosteal surface, the double-labeled surfaces, mineralizing surfaces, and mineral apposition rates were all higher in the OVX compared to the OVX + estrogen group..

Estrogen treatment reduced osteoclastogenesis, stabilized bone turnover, and therefore preserved AB mass in the ovariectomized rat. However, the preservation of AB structure following estrogen treatment remains unclear. Future studies should correlate the preservation of AB structure following ERT with other key sites rich in trabecular bone that are known to respond to ERT in order to place the bone-sparing effects of ERT on AB in the context of systemic bone health.

Table 3: Summary of studies investigating ERT and mandibular health in ovariectomized rats

Rat strain	Sample size per group	Age at OVX (wks)	OVX duration (wks)	Estrogen dose; duration (wks)	Main findings for mandible, compared to OVX	Reference
Wistar	*n* = 4	Unknown	2	17 β-estradiol 1.5 μg/day continuous infusion; 2	•Less nuclei (osteoclasts)	[58]
Sprague-Dawley	*n* = 5	13	7	17 β-estradiol 10 μg/kg 5 days/wk; 7	•36 % less periodontal ligament space	[59]
Wistar	*n* = 14	11	11	17 β-estradiol 20 μg/kg daily; 11	•41 % greater bone density	[30]
Wistar	*n* = 15	26	16	Estriol 100 μg/kg 5 days/wk 12	•Improved Tb.BMD and BMC	[60]
Sprague-Dawley	*n* = 9	13	62	17 β-estradiol 10 μg/kg 4 days/wk; 10	•38 % less periosteal mineralizing surface •88% less endosteal double-labeled surface •51% less endosteal mineralizing surface •71% less endosteal mineral apposition rate	[31]

OVX, ovariectomized; BMD, bone mineral density; BMC, bone mineral content

1.5 Objectives

There are two main study objectives:

1) To quantify the changes to AB structure, density and strength following ERT in the OVX rat, a preclinical model of postmenopausal osteoporosis, using µ-CT.
2) To investigate the relationship between AB structure, density and strength following ERT with trabecular structure and density at the FN and LB3.

The aim of these two objectives is to provide strong preclinical evidence that the effects of ERT on tooth retention in human studies may, at least in part, be explained by the preservation of AB structure. Additionally it will establish the magnitude of the response of AB to ERT in the context of other skeletal sites; such findings will provide an evidence-based rationale for including AB as a potential skeletal site that may be modified by an intervention (i.e. nutritional intervention) targeting trabecular bone.

1.6 Hypotheses

1) ERT will preserve both the structure, density and strength of AB in the ovariectomized rat model as assessed by µ-CT.
2) Preservation of AB will be positively correlated with the known bone-sparing effects of ERT at the FN and LB3.

CHAPTER 2: METHODOLOGY

2.1 Animals

Ovariectomized Sprague Dawley rats (n = 28) were purchased from Charles River Laboratories (Kingston, NY, USA). Prior to arrival, all rats underwent OVX at Charles River at 11 weeks of age. Upon arrival at Brock University, rats were 11 weeks of age and were housed two per cage with a 12:12 hour light/dark cycle and were fed AIN93M (TD.94048; Harlan Teklad, Mississauga, ON, Canada) [57] diet (Table 4) for the duration of the study. This animal study protocol complied with the Canadian Council on Animal Care and was approved by the AUCC at Brock University, St. Catharines, Ontario (AUP # 12-09-01).

Table 4: Composition of AIN93M diet

Ingredient	Amount per kg of diet
Cornstarch	466 g/kg
Casein (≥ 85% protein)	140 g/kg
Dextrinized cornstarch	155 g/kg
Sucrose	100 g/kg
Soy bean oil	40 g/kg
Fiber	50 g/kg
Mineral mix AIN93M	35 g/kg
Calcium	5 g/kg
Vitamin mix AIN93M	10 g/kg
Vitamin D^3	1000 IU/kg
L-Cystine	1.8 g/kg
Choline bitartrate	2.5 g/kg
Tert-butylhydroquinone	0.008 g/kg
Macronutrient summary	
Fat (soybean oil)	40 g/kg (10% total energy)
Protein (purified casein ≥ 85 protein)	126 g/kg (14% total energy)
Carbohydrate (sucrose, cornstarch)	727 g/kg (76% total energy)

2.2 Study design

The ovariectomized rats were randomized into two groups: OVX alone (*n* = 14) or estrogen replacement (*n* = 14). At 12 weeks of age, the estrogen replacement group received a subcutaneous pellet that released 1.5 mg of E2 over 90 days (Innovative Research of America, Sarasota, FL, USA). The ovariectomized control group also received a subcutaneous placebo pellet to compensate for any stress endured during the surgical procedure. All pellets were placed using a trochar into a subcutaneous pocket created above the right scapula region while the rats were under isoflurane anesthesia. After 12 weeks of E2 treatment, both the OVX alone and estrogen replacement groups were euthanized by exsanguination under isoflurane anesthesia. The study design is summarized in Figure 7. The left and right hemimandibles, femurs, and lumbar vertebrae 1-4 were excised, cleaned of soft tissue, wrapped in saline soaked gauze, and stored at -80ºC until further analysis.

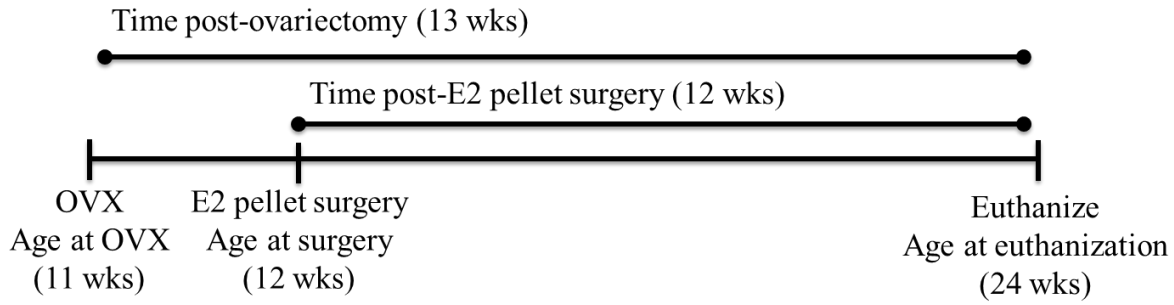

Figure 7: Study design
The rats were OVX at 11 weeks of age. At 12 wks of age, an E2 or placebo pellet was placed. The intervention occurred from 12 through 24 weeks of age. Tissue collection occurred at the end of the 12-week intervention.

2.2.1 E2 dose

The E2 was delivered by a slow release pellet that was implanted subcutaneously. The pellet delivered 1.5 mg E2 over 90-days, resulting in a daily dose of approximately 17 μg of E2 or 50 $\mu g \cdot kg^{-1}$ body weight, assuming an average body weight of 340 g based on previous studies.

2.2.2 Body weight and food intake

Body weight was measured weekly as a marker for overall health. Food intake per cage was measured biweekly. Since the rats were housed two per cage, the cage food intake was divided in half and treated as intake per rat.

2.3 Body composition

One day prior to euthanization, rats were fasted and body composition was measured using dual-energy x-ray absorptiometry (DEXA; pSabre, Orthometrix, Naples, FL, USA) to determine bone, lean, and fat mass. The rats were anesthetized with isoflurane and placed on the DEXA scanning stage in a prone position. The resolution was set at 0.5 x 1.0 cm and the speed at 10 mm/s. Because the area of the rat is larger than the scan field, a ROI was measured using specialized software (Host Software version 3.9.4; Scanner Software version 1.2.0). The ROI was defined by a rectangle 7 cm long and 10 cm wide, beginning at the most proximal aspect of the femoral heads thus excluding the hind limbs. The absolute values for bone, lean, and fat mass were corrected for differences in body mass within the ROI. This was performed by expressing the absolute values as a function of the mass of the ROI and multiplying the value by 100%.

2.4 Scanning skeletal sites by µ-CT

2.4.1 Sample preparation

The right hemimandible, left femur, and LB3 were removed directly from storage at -80ºC and subsequently wrapped in parafilm to prevent sample dehydration during the scan. The wrapped bones were then aligned axially in a foam tube for the scan. By placing multiple samples in a foam tube, the samples were scanned sequentially in batches; this worked to reduce variation due to scanning. An example of the sample set-up is shown in Figure 8.

Figure 8: Sample preparation for µ-CT
A hemimandible removed from -80ºC storage (top). The hemimandible was wrapped in parafilm and placed axially in a foam tube (middle). The foam tube is shown on the scanning platform (used for mice) before entering the scanning field (bottom).

2.4.2 Scanning acquisition and reconstruction parameters

The scanning parameters for the hemimandible, femur, and LB3 were guided by the aim of a minimum sample transmission of 30%. To achieve this aim, the

voltage, current, and filter selection were optimized for each sample type. Additionally, the x-ray exposure time was set to give an average transmission of 60% to yield the best image contrast. The rotation step was set at 0.2º to provide the best resolution while also achieving a manageable scanning duration of approximately 30 minutes per sample. The reconstruction of the individual images into a 3D dataset was also governed by image quality. Due to the density of the cortical bone surrounding the AB, relative to the cortical bone surrounding the FN or lumbar vertebral body, there was more noise in the images of the AB. To compensate, a higher smoothing factor and a defect pixel masking was applied to reduce noise in the AB image slices. All scanning was performed using a Skyscan 1176 µ-CT (Bruker, USA) using host software (1176 version 1.1) and reconstruction software (NRECON version 1.6.6.0). All scans were set as a 180º rotation around the sample with an isotropic voxel size of 9 µm. A summary of the scanning and reconstruction parameters for each site is provided in Table 5.

Table 5: Scanning acquisition and reconstruction parameters for mandible, femoral neck, and lumbar vertebrae

		Mandible	Femoral neck	Lumbar vertebrae
Acquisition parameters				
	Voltage (kV)	82	68	68
	Current (μA)	298	368	368
	Filter	2 mm Al	1 mm Al	1 mm Al
	Exposure (ms)	1254	1140	1140
	Rotation step	0.2º	0.2º	0.2º
Reconstruction parameters				
	Smoothing	4	1	1
	Ring artifact	8	8	8
	Beam hardening	30%	30%	30%
	Defect pixel mask	3%	0%	0%

2.4.3 Mandible positioning and analysis

As seen in Figure 9, each mandible scan was reoriented so that a sagittal slice at M1 exposed a level furcation roof and a frontal slice at the mesial root showed that the root was vertically straight. The images analyzed were the coronal slices passing first through the occlusal surface until the molar root apices.

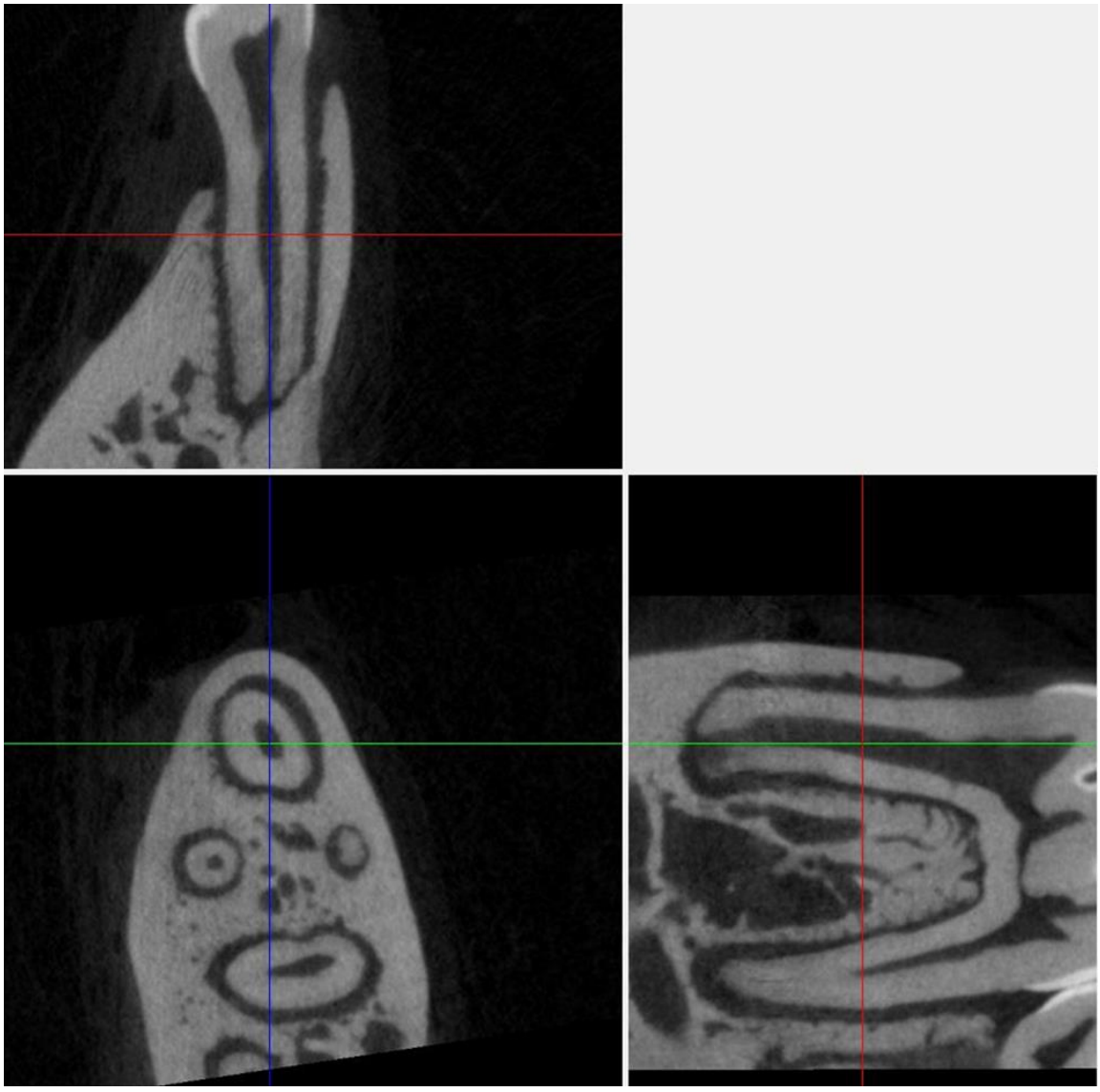

Figure 9: Mandible positioning at M1
A sagittal slice through M1 exposed a level furcation roof (right). A frontal slice through the mesial root showed that the root was aligned vertically (top). The images that were analyzed were the coronal sections proceeding through the AB encased by the four roots of M1 (left).

As seen in Figure 10, the beginning of the ROI was the slice near the furcation roof at which the mesial, distal, lingual, and buccal roots were independent structures

surrounding AB. An interpolated shape was drawn contouring the root surfaces in contact with the AB of the interradicular septum until the end of the mesial root.

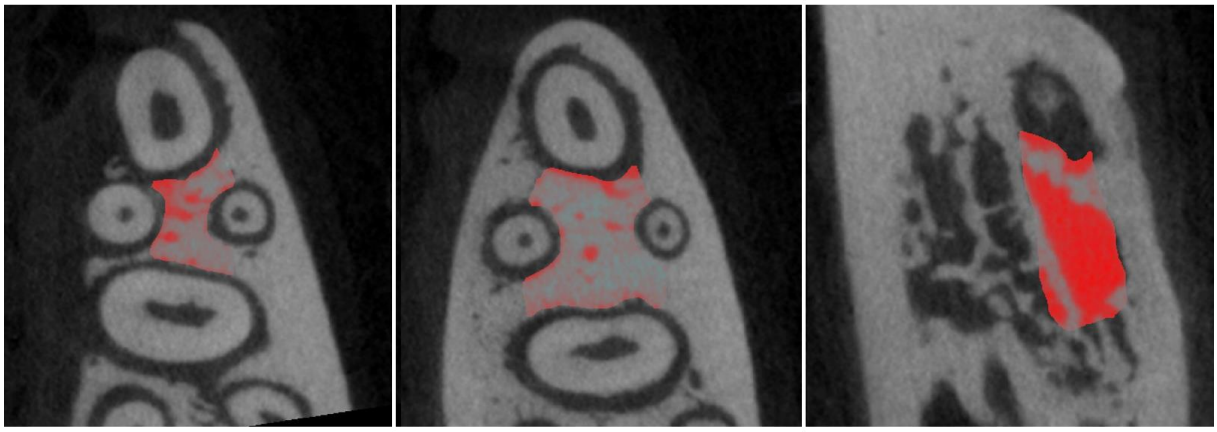

Figure 10: Mandible ROI
The first slice was the point at which all four roots are independent structures (left). The ROI contoured the inner surfaces of the roots to encompass the AB of the interradicular septum (middle). The last slice was the point at which the mesial root ended (right).

As seen in Figure 11 a sub-region of AB between the lingual and buccal roots was also drawn. This sub-region was designed to capture larger trabeculae within the AB and exclude the dense furcation roof for later 3D BMD analysis.

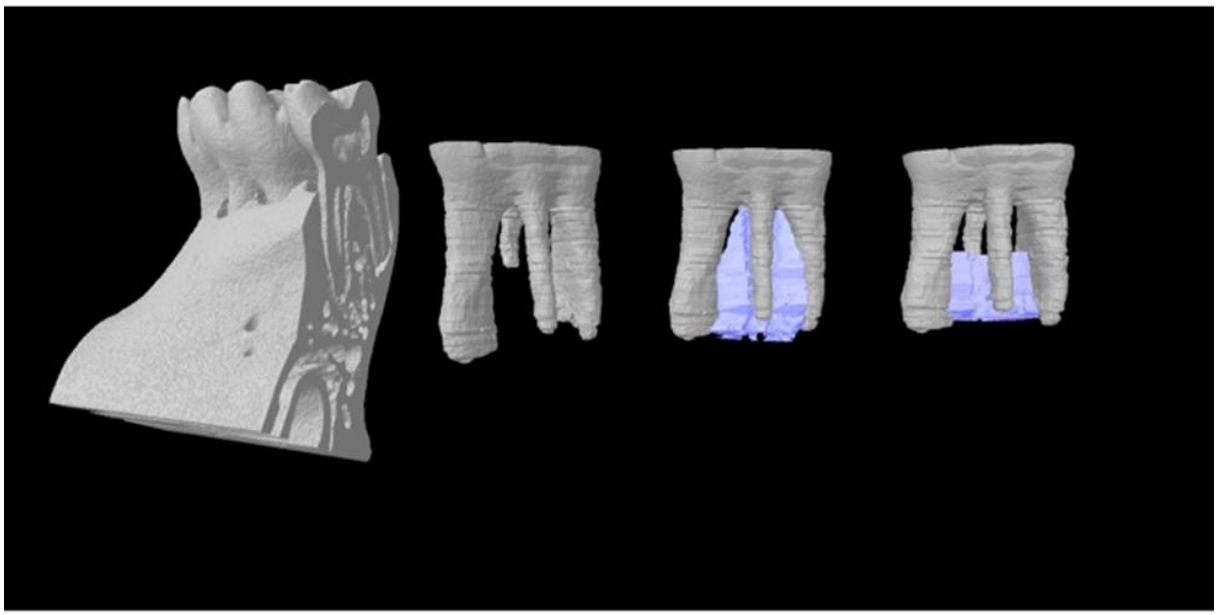

Figure 11: Three-dimensional alveolar bone ROI with sub-region
The entire interradicular septum (light blue; center right) and the AB sub-region between the buccal and lingual roots (light blue; far right)

2.4.4 Femoral neck positioning and analysis

Only the proximal aspect of the femur was scanned in order to image the FN. The FN site was chosen since changes in BMD at the hip in human studies has correlated with an increased likelihood of tooth loss. An aim of this work is to show that a similar relationship exists within the OVX rat model between the FN trabecular bone and AB so that the OVX rat model can be used in future studies targeting both trabecular and AB preservation. As seen in Figure 12, each FN was reoriented so that a sagittal slice exposed the neck aligned horizontally and a coronal slice exposed the neck aligned vertically.

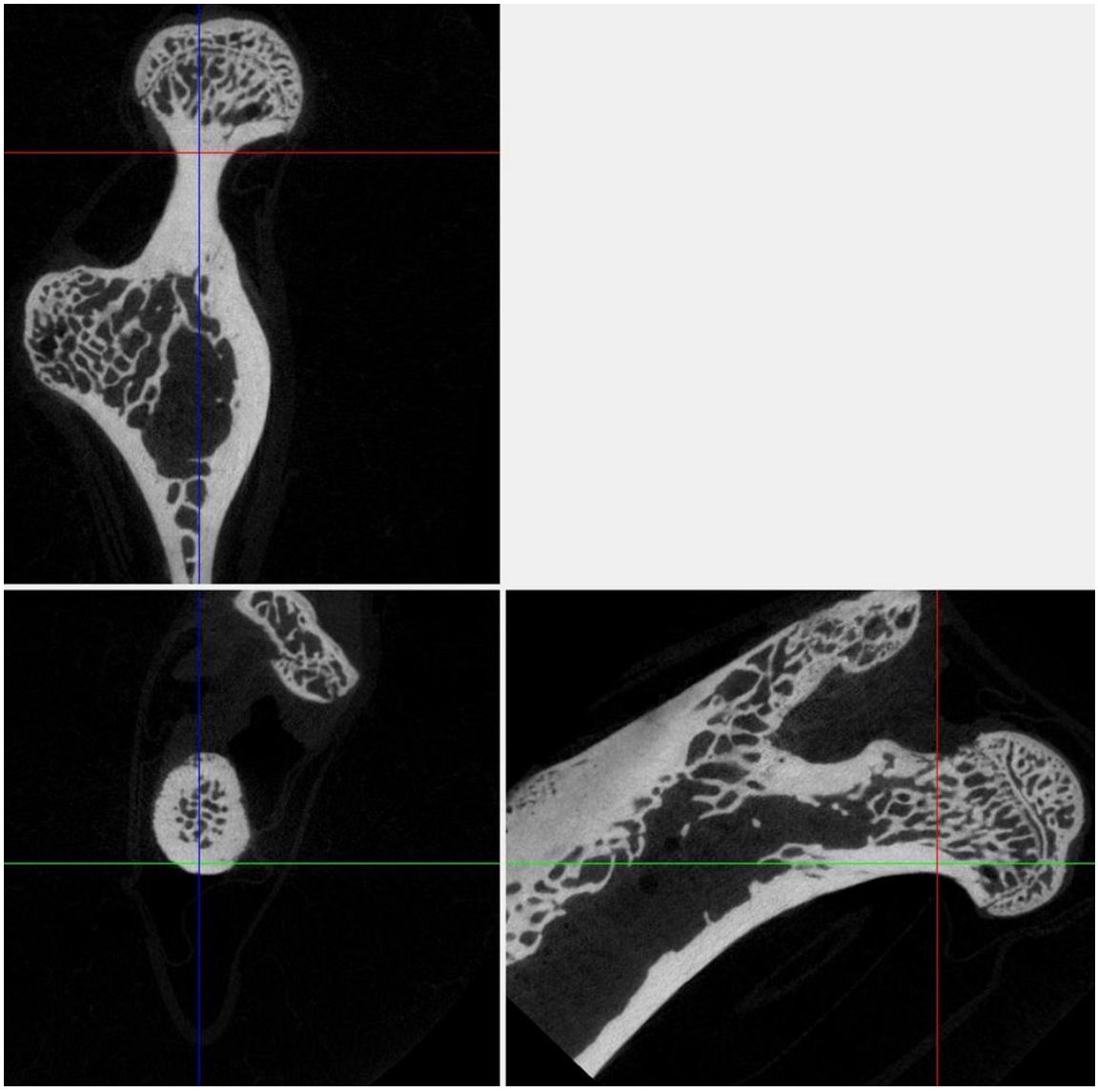

Figure 12: Femoral neck positioning
A sagittal slice exposed a FN that is aligned horizontally (right). A coronal slice exposed a FN that is aligned vertically (top). A frontal slice exposed the trabecular bone within the FN from which an ROI was drawn (left).

The FN ROI began at the last slice to have any femoral head growth plate and continue until the FN became continuous with the main proximal femoral medulla (Figure 13).

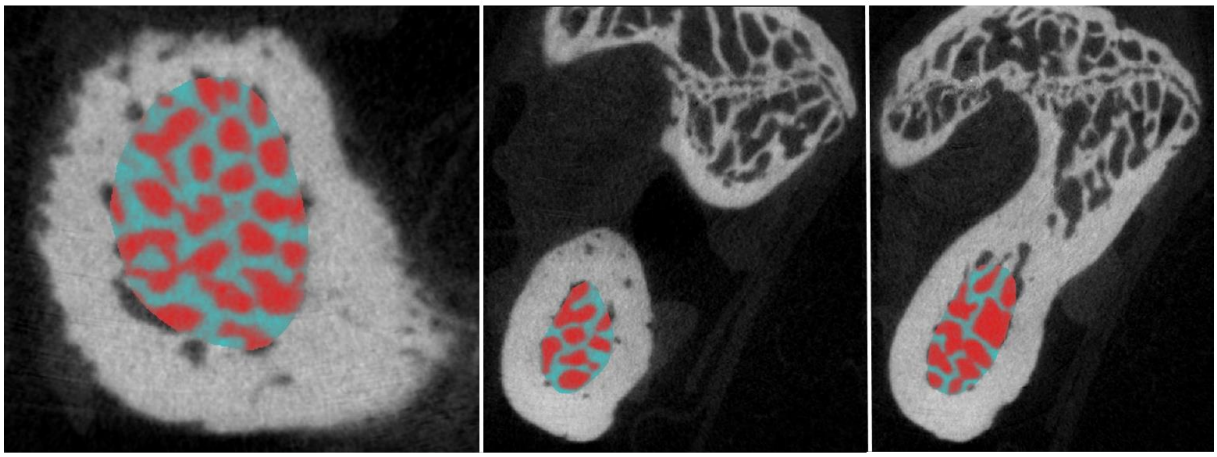

Figure 13: Femoral neck ROI
The first slice of the ROI was the slice after which the femoral head growth place disappeared (left). The ROI continued down the FN (middle). The ROI ended when the FN medulla became continuous with the medulla of the femur (right).

2.4.5 Lumbar vertebrae positioning and analysis

As seen in Figure 14, each LB3 was reoriented so that a sagittal slice exposed a horizontal vertebral body with a vertical, superior, vertebral growth plate, and a coronal slice exposed a vertical vertebral body.

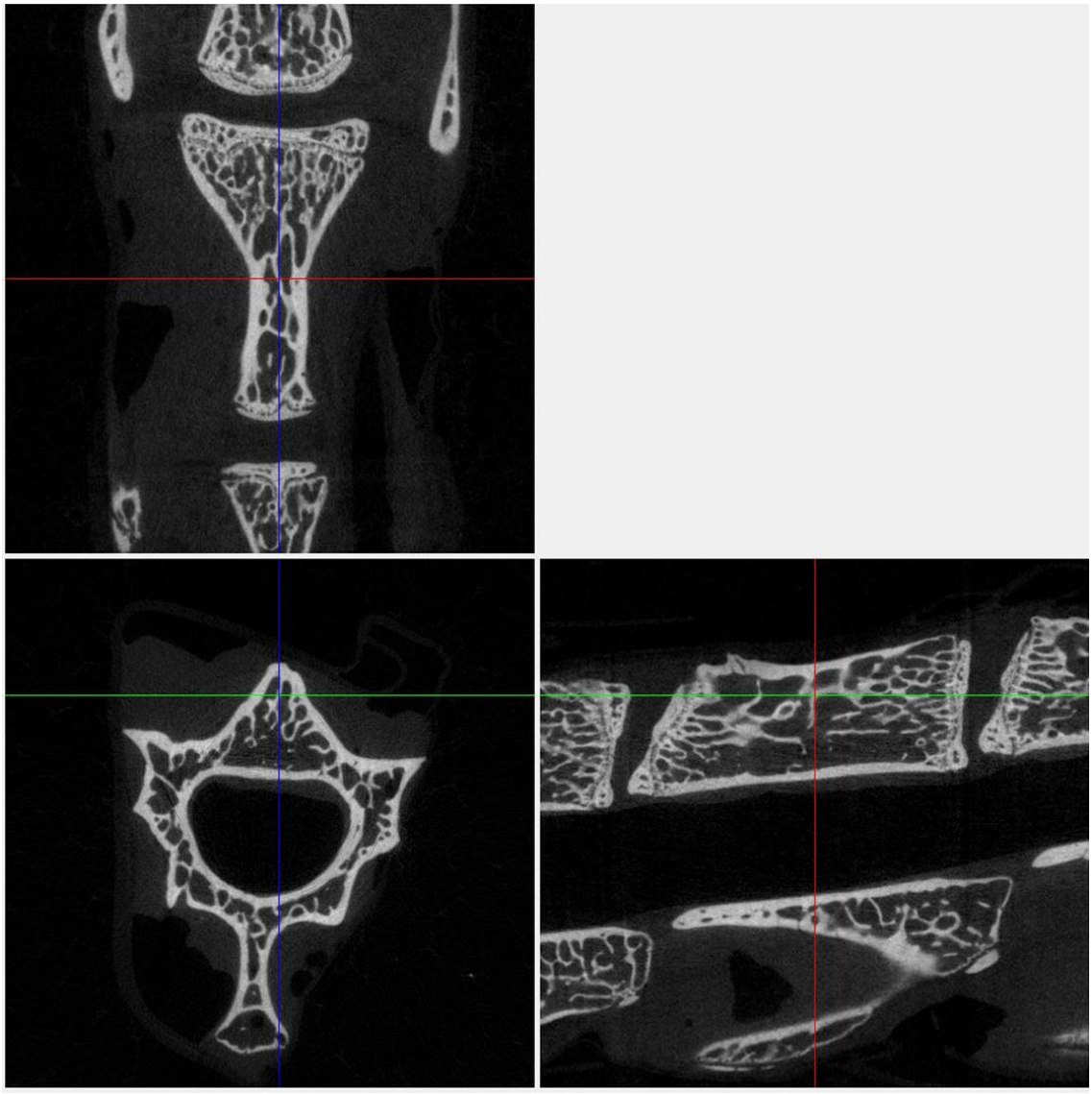

Figure 14: Lumbar vertebrae positioning
A sagittal slice exposed a vertebral body that is aligned horizontally with a superior vertebral growth plate that is aligned vertically (right). A coronal slice exposed a vertebral body that is aligned vertically (top). A frontal slice exposed the trabecular bone of the vertebral body that was used for analysis (left).

The ROI for LB3 was 200 slices; ± 100 slices from the vertebral body midpoint between the two growth plates. A circular primary ROI first captured the entire vertebral body and a secondary manually drawn ROI within the cortical bone of

the vertebral body then isolated the trabecular bone used in the analysis. Figure 15 shows the primary and secondary ROIs.

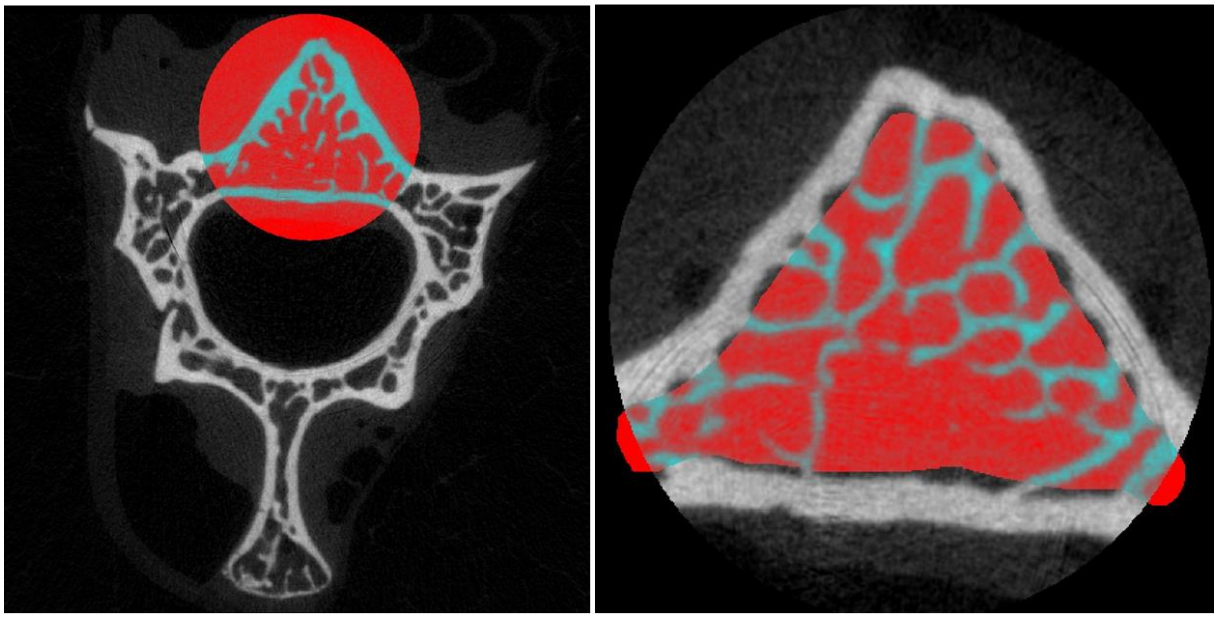

Figure 15: Lumbar vertebrae ROI
A primary ROI isolated the vertebral body from the entire vertebral structure (left). A secondary ROI within the boundaries of the cortical bone captured the trabecular bone for analysis (right).

2.4.6 µ-CT structure and density parameters

A global thresholding model was applied to the ROI of the mandible, FN, and LB3 body to binarize the trabecular bone structure. Then the following structural parameters (described in Table 6) were calculated by the µ-CT specialized software (CTan version 1.13.5.1): BV/TV, Tb.Th, Tb.Sp, Tb.N and the SMI. The 3D BMD was calculated for the entire ROI and was calibrated against hydroxyapatite phantoms in resin that will be described in the next section.

Table 6: Overview of the three-dimensional structural µ-CT parameters

Micro-CT parameter	Interpretation
BV/TV (bone volume/tissue volume)	The percent of bone within your selected ROI
Tb.Th (trabecular thickness)	The width of the trabecular bone in 3D within the ROI
Tb.Sp (trabecular separation)	The width of the space between adjacent trabeculae in 3D within the ROI
Tb.N (trabecular number)	The number of discrete trabeculae in 3D within the ROI
SMI (structural model index)	A surrogate measure for strength specific to the ROI as trabeculae move from the strong plate-like shape to the weaker rod-like shape

2.5 Phantom calibration

The phantom calibrations were performed daily during scanning and consisted of a water phantom in addition to both a low and high density hydroxyapatite phantom. The water phantom was used to calibrate the images for Hounsfield units with air equal to -1000 and water equal to 0. The low and high density hydroxyapatite phantoms, 0.25 $g \cdot cm^{-3}$ and 0.75 $g \cdot cm^{-3}$, respectfully were then used to calibrate Hounsfield units to 3D BMD. An example of the three phantoms in a field of view is shown in Figure 16.

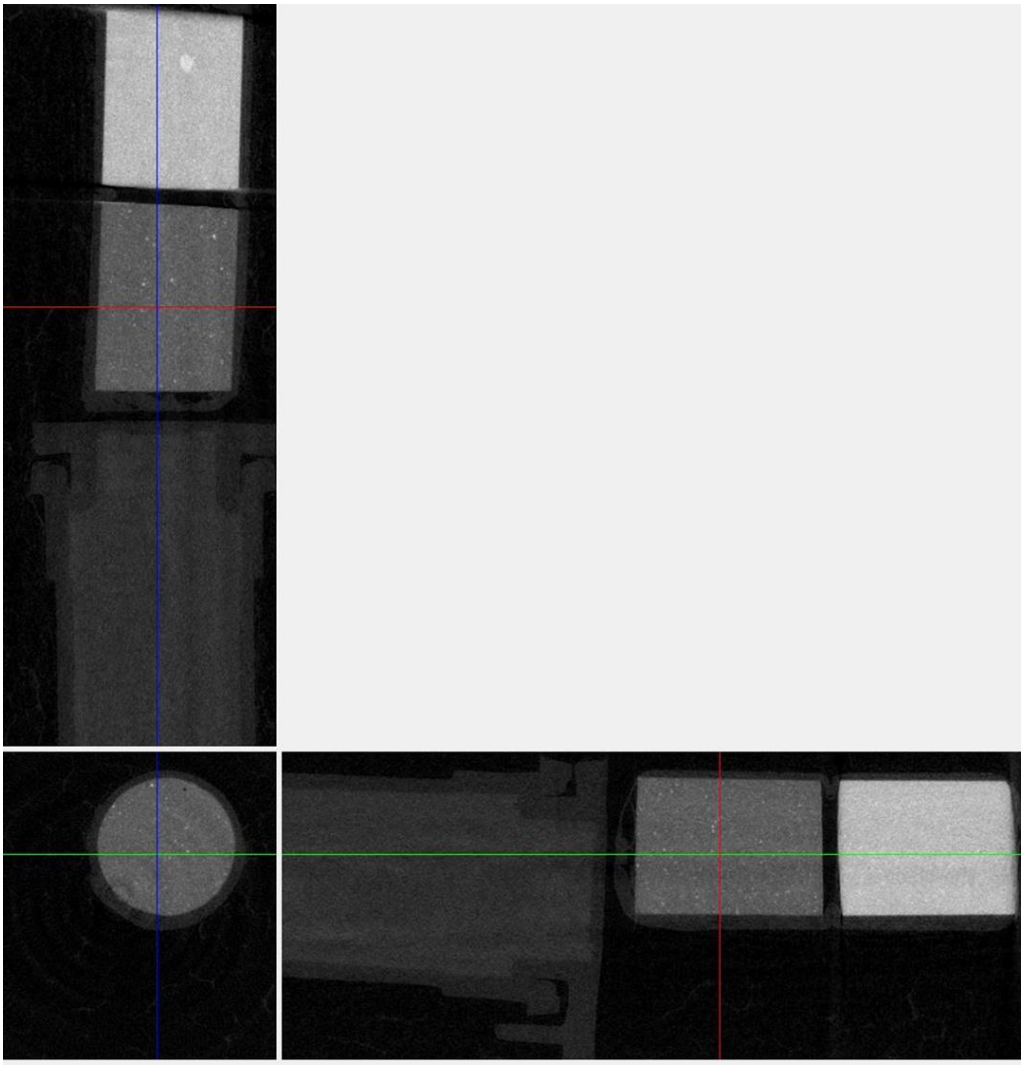

Figure 16: Phantom positioning
The three phantoms used were: a high density phantom (hydroxyapatite in resin 0.75 g·cm^{-3}), a low density phantom (hydroxyapatite in resin 0.25 g·cm^{-3}), and a small PCR tube filled with distilled water (right; sagittal slice), (top; coronal slice). A frontal slice through the low density phantom exposed the surface on which the ROI was drawn for 3D density calibration (left).

2.6 Biomechanical strength testing

The left hemimandibles, left femurs and LB3 were all assessed with biomechanical strength testing (Instron 4442, Norwood, MA, USA) with specialized software (Series IX Automated Materials Tester, version 8.1 5.00). The

hemimandibles were removed from -80ºC, soaked in phosphate buffered saline (PBS) for 2 hours, and then a 3-point bending test was performed. The span width was 10 mm and the hemimandibles were placed buccal side up with the molar occlusal surface facing the operator (Figure 17). The crosshead speed was 2 mm/min and peak load was measured.

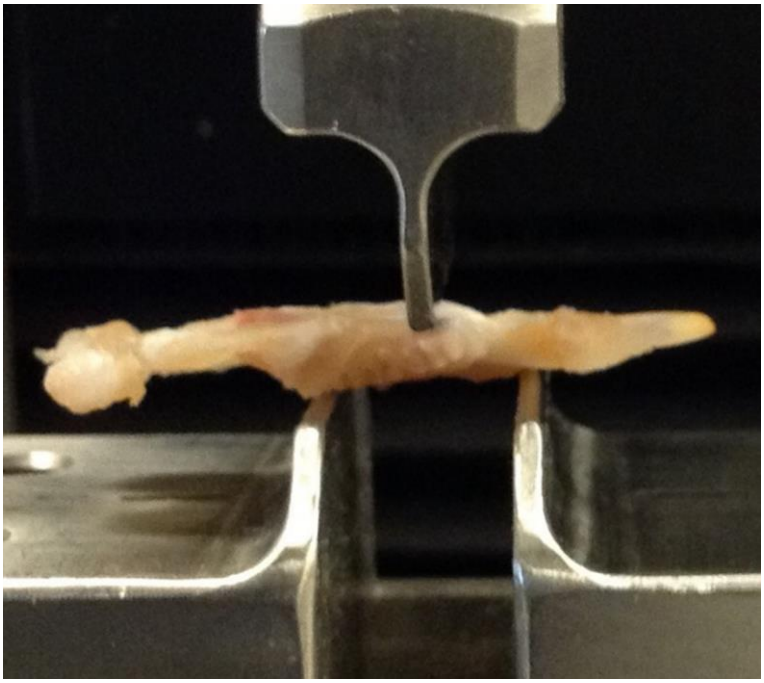

Figure 17: Biomechanical strength testing of mandible
The left hemimandible was positioned buccal side facing up, across a span width of 10 mm, with the crosshead at the midpoint of M1.

The femurs were removed from -80ºC, soaked in PBS for 2 hours, and then the 3-point bending test was performed. The span width was 15 mm and the femur was placed with the anterior surface facing up. The crosshead speed was 2 mm/min and peak load was measured.

Each LB3 was removed from -80ºC, soaked in PBS for 2 hours, and had the spinous processes trimmed prior to strength testing. The LB3 was placed on a bottom

steel head with the cranial vertebral body surface facing up. A top steel head then came into contact with the cranial vertebral body surface to measure peak load before compressive failure.

2.7 Areal BMD and BMC of mandible, femur, and LB1-4 by DEXA

The left hemimandibles were removed from -80ºC and immediately scanned with DEXA (Host software 3.9.4/1.2.0, analysis software version 3.9.4). The scanning resolution was 0.2 x 0.2 mm with a 5 mm/s scanning speed. A left hemimandible (estrogen group, rat #6) was scanned 3 times without repositioning and the percent coefficients of variation for whole BMD and BMC were 0.10% and 0.79%, respectively. The left femurs were removed from -80 ºC and immediately scanned with DEXA. The scanning resolution was 0.2 x 0.2 mm with a 10 mm/s scanning speed. A left femur (OVX group, rat #14) was scanned 5 times without repositioning and the coefficients of variation for the whole BMD and BMC were 0.68% and 0.73% respectively. Lumbar vertebrae 1 through 4 (LB1-4) were removed from -80ºC and immediately scanned with DEXA. The scanning resolution was 0.2 x 0.2 mm with a 10 mm/s scanning speed. LB1-4 from the OVX group, rat #14 were scanned 5 times without repositioning and the coefficients of variation for the whole BMC and BMC were 0.52% and 0.47% respectively.

2.8 Plasma measures of bone remodeling

Fasted blood samples were collected from the rats under isoflurane anesthesia from the tail vein into EDTA coated tubes. The blood was immediately centrifuged at 2000 x g for 10 minutes at 4ºC and the plasma was aliquoted for storage at -80ºC until analysis. Plasma measure of: receptor activator of nuclear factor kappa-B ligand

(RANKL), osteoprotegrin (OPG), parathyroid hormone (PTH), osteocalcin, insulin, and leptin were obtained using Magpix immunobead assay technology with xPONENT software (Luminex Corp., Austin, TX, USA). The kits used were as follows:

- Milliplex MAP Rat RANKL Single Plex Magnetic Bead Kit (RRNKLMAG-31K-01; Millipore Corp., Billerica, MA, USA)
- Milliplex MAP Rat Osteocalcin Single Plex Magnetic Bead Kit (RBNMAG-31K-1OC; Millipore Corp., Billerica, MA, USA)
- Milliplex MAP Rat Bone Panel 2 Magnetic Bead Kit (RBN2MAG-31K; Millipore Corp., Billerica, MA, USA)

2.9 Statistical analysis

The group body weights and food intake were first analyzed with a D'Agostino & Pearson omnibus normality test and were then compared with a two-way ANOVA. This design accounts for the effects of time and between-group differences on body weight and food intake.

The 3D structure and density parameters (BV/TV, Tb.N, Tb.Th, Tb.Sp, SMI and BMD) for each group were first assessed for normality with D'Agostino & Pearson omnibus normality test and then compared between groups at each site with a parametric or non-parametric t-test.

To investigate the relationship between AB 3D structure and systemic trabecular bone 3D structure, the μ-CT parameters (BV/TV, Tb.N, Tb.Th, Tb.Sp, SMI and BMD) were correlated among the mandible, FN, and LB3 body. The groups

were first assessed for normality with D'Agostino & Pearson omnibus normality test and then were analyzed with a Pearson or Spearman correlation test.

Group site morphometrics (sample weight, length, height), peak loads and areal BMD/BMC were first assessed for normality with a D'Agostino & Pearson omnibus normality test and then were compared between groups at each site with a parametric or non-parametric t-test.

The group plasma measures (RANKL, OPG, PTH, osteocalcin, insulin, and leptin) were first assessed for normality with D'Agostino & Pearson omnibus normality test and then were compared with a parametric or non-parametric t-test. To investigate the response of AB to plasma measures of bone remodeling, in reference to the well characterized sites of the FN and LB3 body, the BV/TV of the mandible, FN, and LB3 body was each correlated with plasma: RANKL, OPG, PTH, osteocalcin, insulin, and leptin.

CHAPTER 3: RESULTS

3.1 Body weight and food intake during the 12 week E2 intervention

There was an interaction between time and the E2 intervention on the difference between group body weights ($P < 0.0001$). Additionally both time ($P < 0.0001$) and the intervention ($P < 0.05$) each explained a significant amount of the variation in body weight. At week 2 ($P < 0.01$) and weeks 3-4 ($P < 0.05$) the average body weight of the OVX group was higher than the E2 group. From weeks 5-12 there was no difference in average body weight between the OVX and E2 groups (Figure 18 A). There was an interaction between time and E2 intervention for the difference between group food intake ($P < 0.0001$). Time alone ($P < 0.0001$) explained a significant amount of the variation in the food intake of both groups, but no additional variation was explained based on the E2 intervention. Only at one week after the E2 pellet placement did the E2 group have a reduced food intake compared to the OVX group ($P < 0.0001$). There was no difference in food intake between the OVX and E2 groups from weeks 2-12. (Figure 18 B).

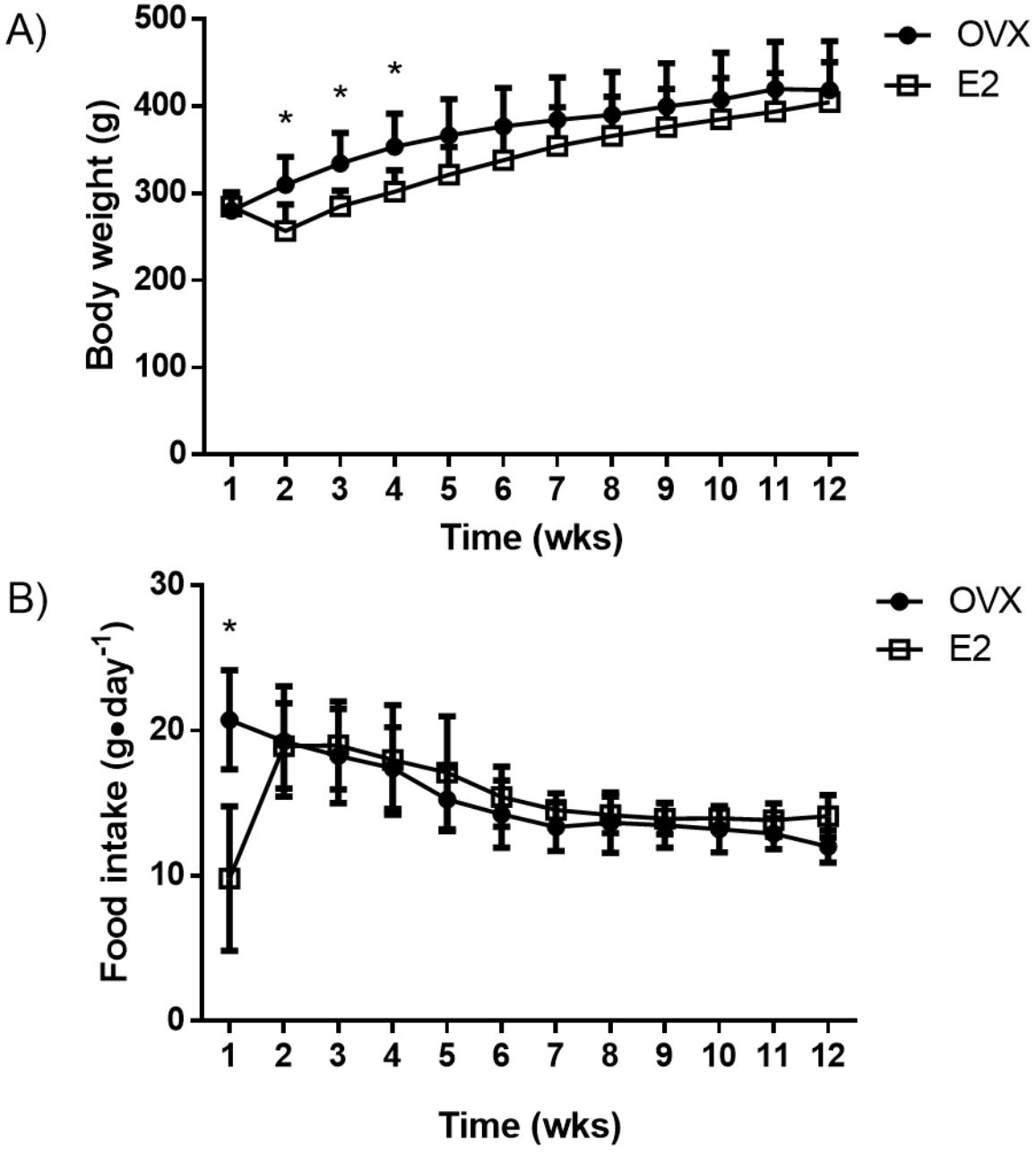

Figure 18: Body weight and food intake
A) Average body weights and B) Average food intake for each group at weekly intervals.
Results expressed as the mean ± SD
Differences between OVX and E2: $^{*}P < 0.05$
n = 10-14 per group for body weight and food intake

3.2 Regional body composition at the end of the 12 week E2 intervention

At the end of the 12 week E2 intervention, the E2 group had greater areal BMD compared to the OVX group and there were no differences in BMC, lean mass, or fat mass (Table 7).

Table 7: Regional body composition at the end of the 12 week E2 intervention

	OVX	E2
BMD ($g \cdot cm^{-2}$)	0.13 ± 0.02	0.15 ± 0.03[a]
BMC (g)	2.6 ± 0.6	2.30 ± 0.7
Standardized to ROI (%)	1.7 ± 0.3	1.5 ± 0.3
Lean mass (g)	73.8 ± 11.0	80.1 ± 15.1
Standardized to ROI (%)	50.1 ± 12.6	55.2 ± 15.5
Fat mass (g)	75.3 ± 28.2	67.2 ± 31.6
Standardized to ROI (%)	48.3 ± 12.4	43.3 ± 15.3

Results expressed as the mean ± SD
OVX, ovariectomized; E2, estrogen replacement
Differences between OVX and E2 within sites: [a] $P < 0.05$
$n = 14$ per group

3.3 µ-CT structure and density of alveolar bone at mandible, and trabecular bone at femoral neck and lumbar vertebrae

AB of the E2 group had greater BV/TV ($P < 0.001$), Tb.N ($P < 0.05$), and Tb.Th ($P < 0.01$) compared to the OVX group while AB of the OVX group had greater Tb.Sp ($P < 0.01$) and SMI ($P < 0.001$) compared to the E2 group. Alveolar BMD of the E2 group was not greater than the OVX group BMD ($P = 0.09$). BV/TV, Tb.N, and BMD ($P < 0.001$) of the FN and LB3 was greater in the E2 group compared to the OVX group. Tb.Sp and SMI were higher ($P < 0.001$) at both the FN and LB3 in the OVX group compared to the E2 group. There was no difference in Tb.Th at the FN or LB3 between the OVX and E2 groups (Table 8).

Table 8: Structure and density of alveolar bone of mandible, trabecular bone at the femoral neck, and trabecular bone at the lumbar vertebral body

	Mandible		FN		LB3	
	OVX	E2	OVX	E2	OVX	E2
BV/TV (%)	62.32 ± 5.03	72.10 ± 4.33[c]	49.16 ± 4.99	61.12 ± 6.60[c]	23.19 ± 3.11	34.66 ± 3.81[c]
Tb.N (mm^{-1})	2.35 ± 0.15	2.52 ± 0.20[a]	3.70 ± 0.31	4.36 ± 0.34[c]	2.29 ± 0.28	3.31 ± 0.28[c]
Tb.Th (mm)	0.27 ± 0.02	0.29 ± 0.03[b]	0.13 ± 0.01	0.14 ± 0.02	0.10 ± 0.01	0.11 ± 0.01
Tb.Sp (mm)	0.29 ± 0.06[b]	0.21 ± 0.06	0.21 ± 0.03[c]	0.16 ± 0.02	0.33 ± 0.04[c]	0.24 ± 0.03
SMI	0.15 ± 0.37[c]	- 0.96 ± 0.58	0.55 ± 0.30[c]	- 0.89 ± 0.69	1.34 ± 0.23[c]	0.52 ± 0.27
BMD ($g \cdot cm^{-3}$)	0.26 ± 0.09	0.33 ± 0.10	0.50 ± 0.07	0.67 ± 0.09[c]	0.15 ± 0.06	0.32 ± 0.06[c]

Results expressed as the mean ± SD

OVX, ovariectomized; E2, estrogen replacement; BV/TV, percent BV; Tb.N, trabecular number; Tb.Th, trabecular thickness; Tb.Sp, trabecular separation; SMI, structure model index; BMD, BMD

Differences between OVX and E2 within sites: [a] $P < 0.05$; [b] $P < 0.01$; [c] $P < 0.001$

$n = 14$ per group

3.3.1 Three-dimensional imaging of alveolar bone in the mandible

Representative alveolar regions (based on BV/TV) are shown in Figure 19. Specifically, the average alveolar region BV/TV in the OVX group was 62.32 % and the closest rat alveolar region was OVX rat #2 with a BV/TV of 61.78%. The average alveolar region BV/TV in the E2 group was 72.10% and the closest rat alveolar region was E2 rat #12 with a BV/TV of 71.74%. The alveolar region ROI from OVX #2 and E2 #12 are shown in Figure 19 from an inferior view looking up to the furcation roof of M1.

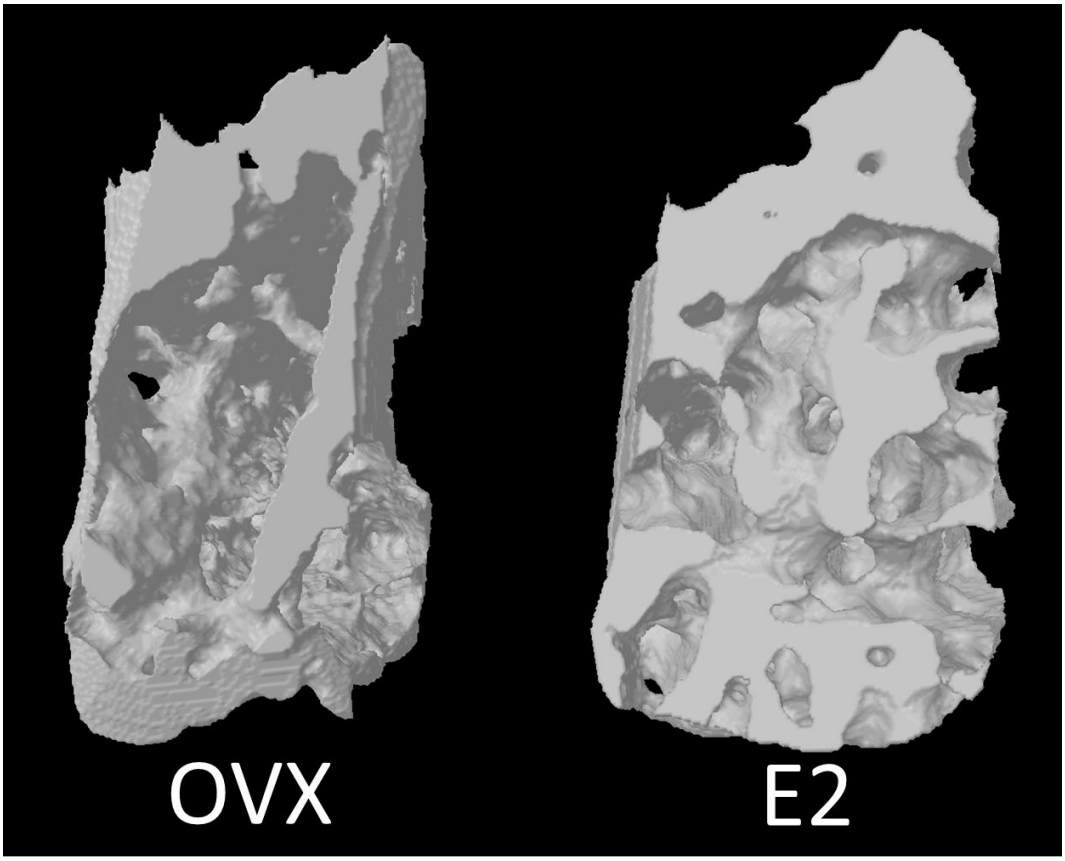

Figure 19: Representative three-dimensional models of alveolar bone from OVX and E2 treated rats
The alveolar region from the OVX group represents a BV/TV of 61.78% while the region from the E2 group represents a BV/TV of 71.74%.

3.3.2 Three-dimensional imaging of femoral neck region

Representative FN regions (based on BV/TV) are shown in Figure 20. Specifically, the average BV/TV for the OVX group FN was 49.16% and the rat with the closest BV/TV was OVX rat #2 at 48.07%. The average BV/TV for the E2 group FN was 61.12% and the rat with the closest BV/TV was E2 rat #13 at 61.17%. The 3D FN ROI of OVX rat #2 and E2 rat #13 are shown in Figure 20 from a superior view beginning at the most proximal aspect of the neck, near the base of the femur head.

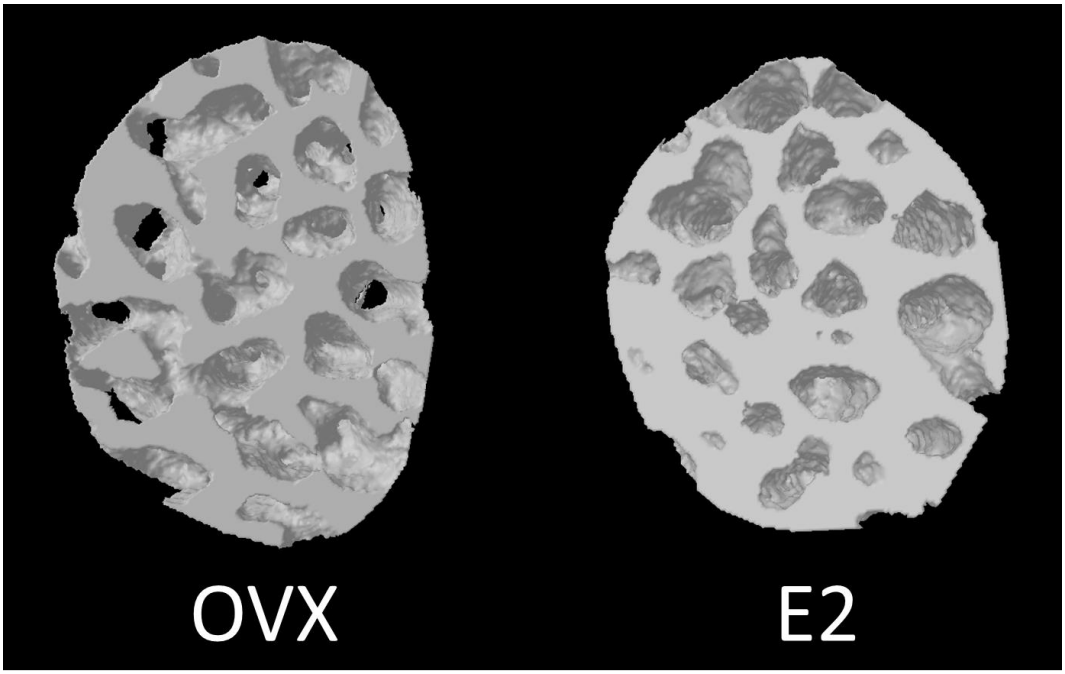

Figure 20: Representative three-dimensional models of the femoral neck region from OVX and E2 treated rats
The FN region from the OVX group represents a BV/TV of 48.07% while the region from the E2 group represents a BV/TV of 61.17%.

3.3.3 Three-dimensional imaging of lumbar vertebrae region

Representative lumbar vertebral body regions (based on BV/TV) are shown in Figure 21. Specifically, the average BV/TV for the OVX group LB3 region was 23.19% and the rat with the closest BV/TV was OVX rat # 5 at 22.83%. The average BV/TV for the E2 group LB3 region was 34.66% and the rat with the closest BV/TV was E2 rat # 8 at 35.05%. The 3D LB3 region of OVX rat #5 and E2 rat #8 are shown in Figure 21 from a superior view.

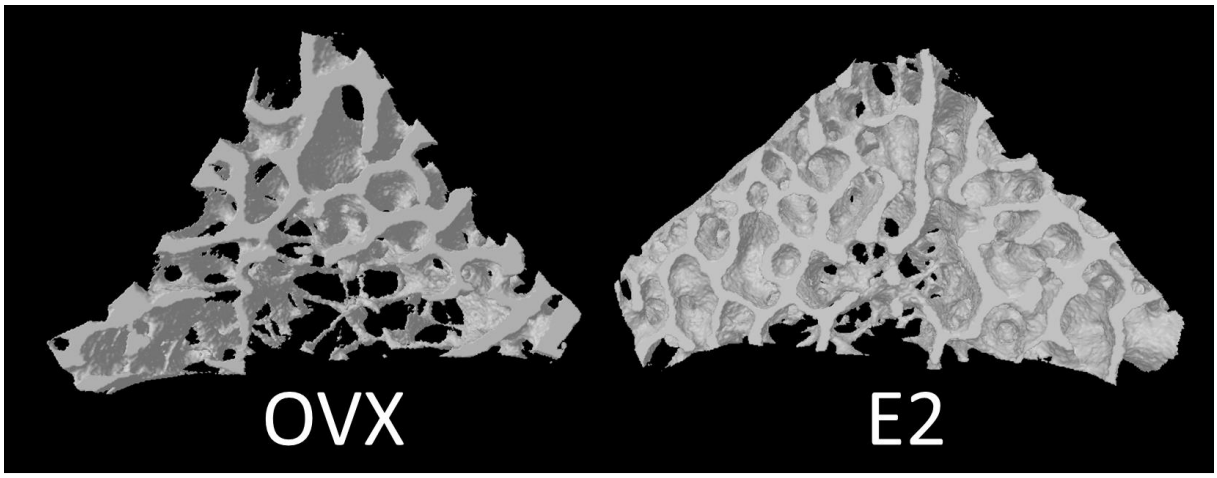

Figure 21: Representative three-dimensional models of the lumbar vertebrae region from OVX and E2 treated rats
The LB3 region from the OVX group represents a BV/TV of 22.83% while the region from the E2 group represents a BV/TV of 35.05%.

3.3.4 Three-dimensional imaging of mandibular alveolar bone, femoral neck and lumbar vertebrae regions

Figure 22 shows all of the representative 3D ROI in one image to facilitate simultaneous comparison across the multiple sites and between study groups. The E2 treated ROI appear denser, with smaller marrow spaces, and better connected trabeculae.

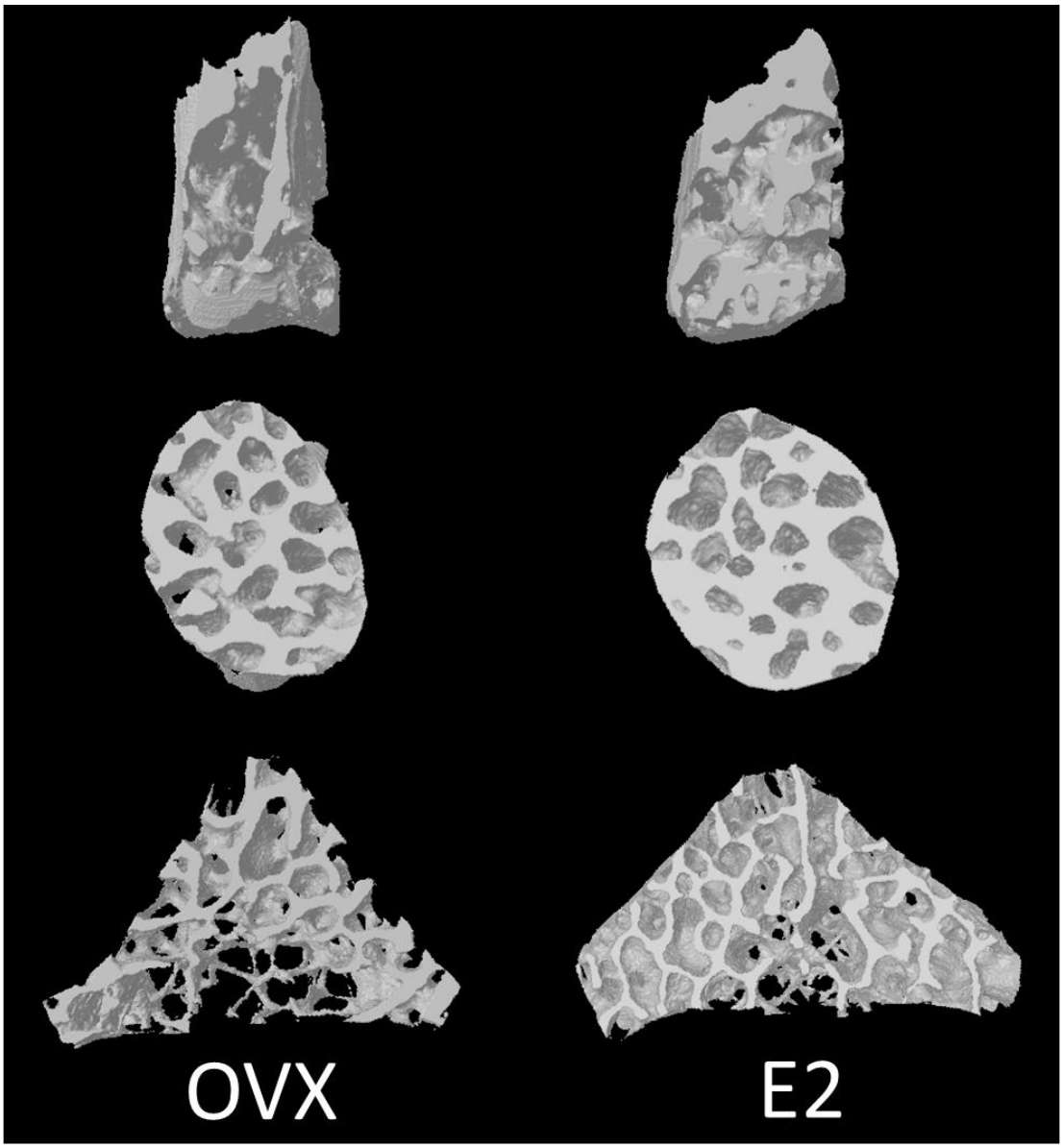

Figure 22: Representative three-dimensional models of mandibular alveolar, femoral neck, and lumbar vertebrae regions of OVX and E2 treated rats
The alveolar, FN, and lumbar vertebrae regions (top to bottom) of the OVX (left) and E2 (right) treated rats.

3.4 Microarchitecture and density of the alveolar bone sub-region as assessed by µ-CT

In a sub-region of AB between the apices of the M1 lingual and buccal roots there was a greater BV/TV, Tb.Th, ($P < 0.001$) and BMD ($P < 0.05$) in the E2 group compared to the OVX group. The OVX group had a greater Tb.Sp ($P < 0.01$) and SMI ($P < 0.001$) compared to the E2 group. There was no difference in Tb.N in the sub-region of AB between the OVX and E2 groups (Figure 23).

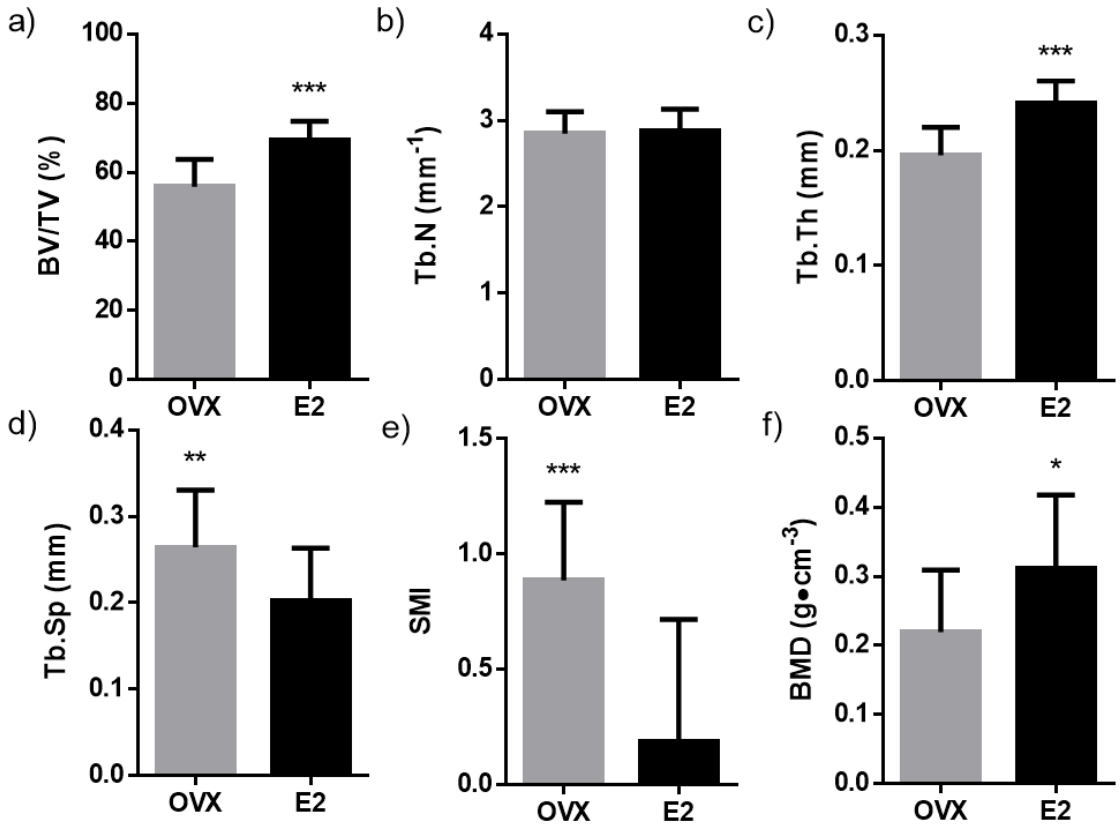

Figure 23: Microarchitectural and density differences in the alveolar bone sub-region between OVX and E2 treated rats
Structure and density parameters from µ-CT of AB sub-region.
A) BV/TV, B) Tb.N, C) Tb.Th, D) Tb.Sp, D) SMI, E) BMD
$^{*}P < 0.05$; $^{**}P < 0.01$; $^{***}P < 0.001$
$n = 14$ per group

3.4.1 Three-dimensional imaging of the mandibular alveolar bone sub-region

The alveolar sub-region contains only the AB found between the apices of the lingual and buccal roots. The sub-regions are from OVX rat #2 and E2 rat # 12 with a BV/TV of 54.58% and 72.96%. The sub-regions selected were from the rats with the closest average BV/TV to the entire alveolar region, and not from those with the closest BV/TV to the average alveolar sub-region. This facilitates a direct comparison between the entire alveolar region (Figure 19) and the alveolar sub-region within the same rats (Figure 24).

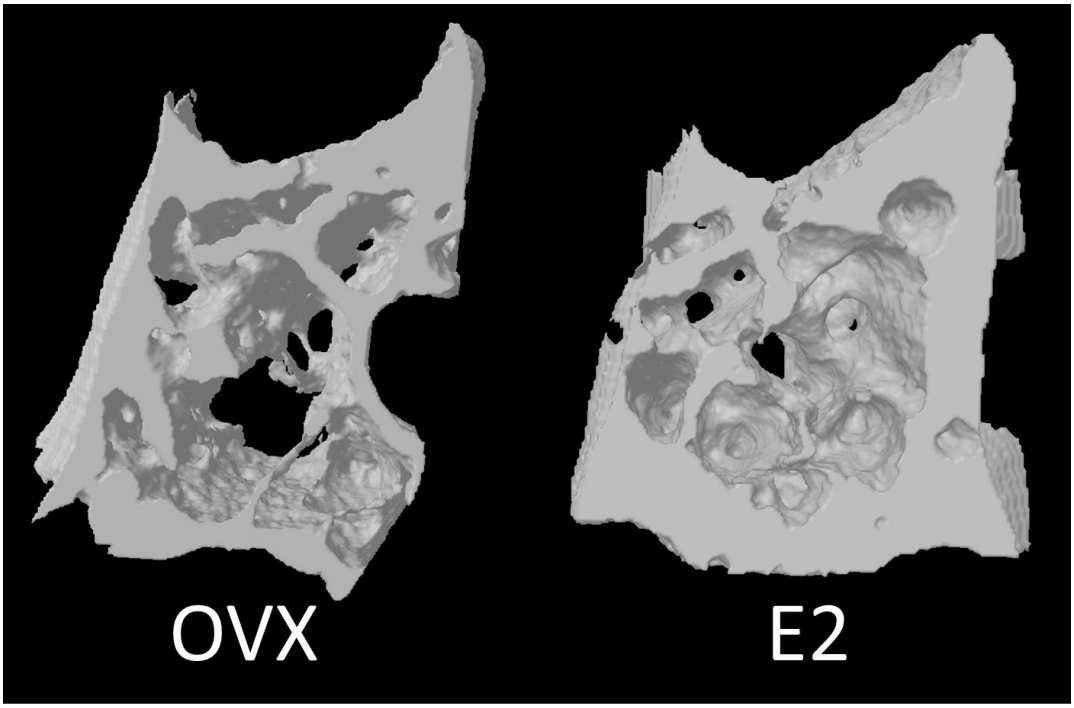

Figure 24: Representative three-dimensional models of the alveolar sub-region of OVX and E2 treated rats
The alveolar sub-region from the OVX group represents a BV/TV of 54.58% while the sub-region from the E2 group represents a BV/TV of 72.96%.

3.5 Correlation among outcomes of alveolar and trabecular bone of the femoral neck, and lumbar vertebral body measured by µ-CT

There was a positive correlation among the BV/TV, Tb.N, Tb.Sp, and SMI of the AB region and the BV/TV, Tb.N, Tb.Sp, and SMI of both the FN or LB3. There was no correlation between the Tb.Th or BMD of the AB region and the FN. However, there was a positive correlation between the Tb.Th and BMD of the AB region and the LB3 (Table 9).

Table 9: Correlation among outcomes of alveolar and trabecular bone of the femoral neck or lumbar vertebrae measured by µ-CT

	FN		LB3	
AB	*r*	*P*	*r*	*P*
BV/TV (%)	0.69	< 0.0001	0.75	< 0.0001
Tb.N (mm^{-1})	0.42	< 0.05	0.44	< 0.05
Tb.Th (mm)	0.21	NS	0.42	< 0.05
Tb.Sp (mm)	0.49	< 0.01	0.63	< 0.001
SMI	0.73	< 0.0001	0.69	< 0.0001
BMD ($g \cdot cm^{-3}$)	0.28	NS	0.47	< 0.05

BV/TV, percent BV; Tb.N, trabecular number; Tb.Th, trabecular thickness; Tb.Sp, trabecular separation; SMI, structure model index; BMD, BMD
n = 14 per group

In order to show the clustering of data points between the groups for BV/TV, Tb.N, Tb.Sp, and SMI the correlation plots are shown in Figure 25.

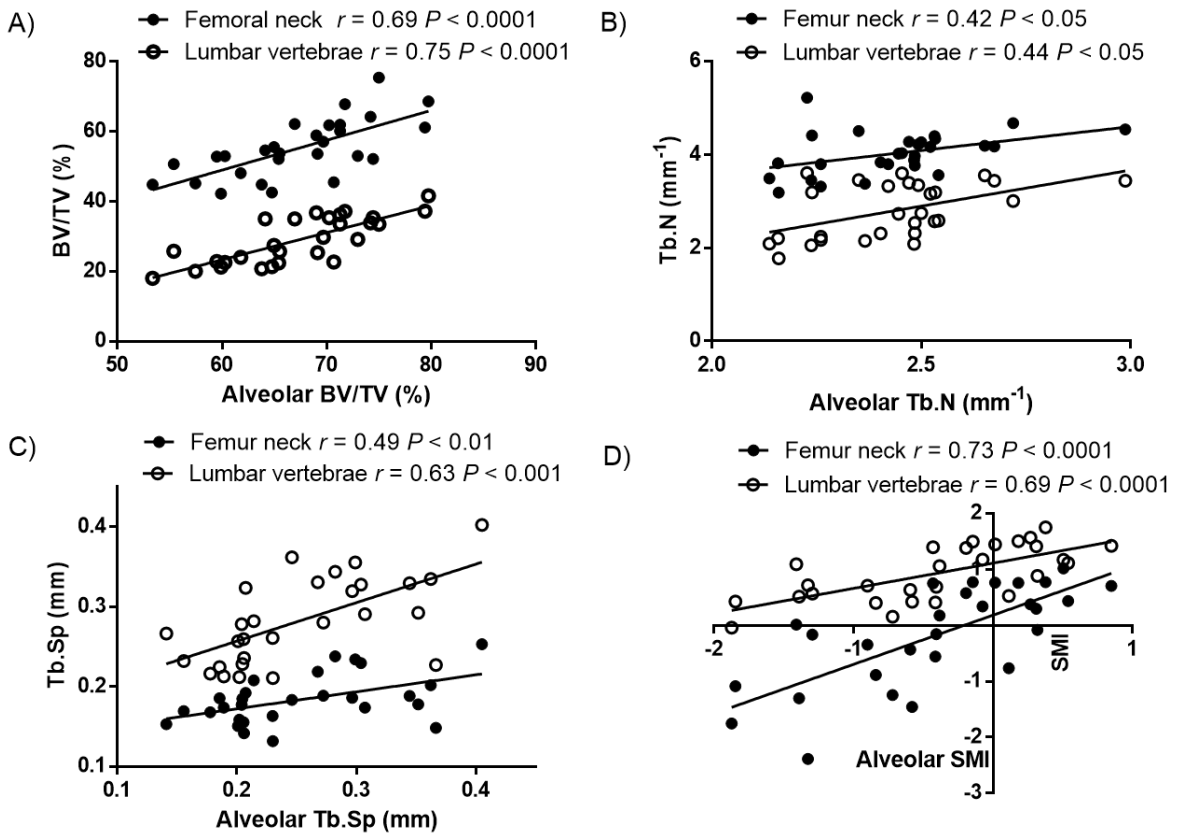

Figure 25: Correlation plots for structural outcomes between mandible and femoral neck or lumbar vertebrae measured by u-CT.
Correlation plots showing the data distributions for A) BV/TV, B) Tb.Th, C) Tb.Sp, D) SMI.
n = 28 per site

3.6 Biomechanical strength testing and DEXA of mandible, femur, and LB1-4 (LB3 only for strength testing)

The OVX hemimandibles were heavier and withstood a greater peak load before fracture than the hemimandibles from the E2 group. The hemimandibles of the OVX group also had a greater whole BMD and BMC than the hemimandibles of the E2 group. There was no difference in femoral weight or length between the groups. The femurs from the OVX group withstood a greater peak load before fracture than the femurs from the E2 group despite the femurs from the E2 group having a greater

areal BMD. There was no difference in femur areal BMC between the groups. There was also no difference in LB3 weight between the groups despite the greater height of the LB3 from the OVX group compared to the LB3 form the E2 group. No differences in LB3 peak load to compressive failure between the groups was detected even though the LB3 from the E2 group had a greater areal BMD. There was no difference in LB3 areal BMC between the groups (Table 10).

Table 10: Peak load by biomechanical strength testing and areal BMC and BMD by DEXA for mandible, femur, and lumbar vertebrae

		OVX	E2
Peak load by a materials testing system:			
Mandible			
	Weight (g)	0.72 ± 0.05[a]	0.67 ± 0.06
	Peak load (N)	141 ± 14[a]	128 ± 12
Femur			
	Weight (g)	1.09 ± 0.09	1.05 ± 0.08
	Length (mm)	37.3 ± 1.1	36.6 ± 0.7
	Peak load (N)	154 ± 19[c]	128 ± 12
Lumbar Vertebrae			
	Weight (g)	0.60 ± 0.10	0.59 ± 0.07
	Height (mm)	8.3 ± 0.5[a]	7.9 ± 0.4
	Peak load (N)	330 ± 29	305 ± 67
Areal BMD and BMC by DEXA:			
Whole mandible			
	BMD (g cm^{-2})	0.16 ± 0.01[a]	0.15 ± 0.01
	BMC (g)	0.36 ± 0.02[c]	0.33 ± 0.02
Whole femur			
	BMD (g cm^{-2})	0.22 ± 0.01	0.23 ± 0.02[a]
	BMC (g)	0.44 ± 0.03	0.45 ± 0.04
Lumbar vertebrae			
	BMD (g cm^{-2})	0.20 ± 0.01	0.21 ± 0.02[b]
	BMC (g)	0.47 ± 0.05	0.50 ± 0.06

Results expressed as the mean ± SD
OVX, ovariectomized; E2, estrogen replacement
Differences between OVX and E2 within sites: [a] $P < 0.05$; [b] $P < 0.01$; [c] $P < 0.001$
n = 12-14 per group

3.7 Plasma measures of bone remodeling

There were no differences in plasma RANKL, OPG, PTH, osteocalcin, insulin or leptin between the OVX and E2 groups (Table 11).

Table 11: Plasma measures of bone remodeling

Analytes (pg ml^{-1})	OVX	E2	P value
RANKL	29 ± 10	23 ± 11	0.08
OPG	679 ± 390	767 ± 511	0.45
Osteocalcin	83 ± 38	94 ± 51	0.55
Insulin	681 ± 438	679 ± 490	0.82
Leptin	6682 ± 2324	7119 ± 4409	0.71
PTH	87 ± 30	67 ± 32	0.10

Results expressed as the mean ± SD
OVX, ovariectomized; E2, estrogen replacement
n = 13-14 per group

3.8 Correlation among plasma measurements of bone remodeling and BV/TV at mandible, femoral neck and lumbar vertebrae

There was a negative correlation between plasma RANKL concentration and BV/TV at the FN and LB3 but not at the mandible ($P = 0.11$) (Figure 26 A). There was also a negative correlation between plasma PTH concentration and BV/TV at the LB3 but not at the mandible ($P = 0.09$) and FN ($P = 0.08$) (Figure 26 B).

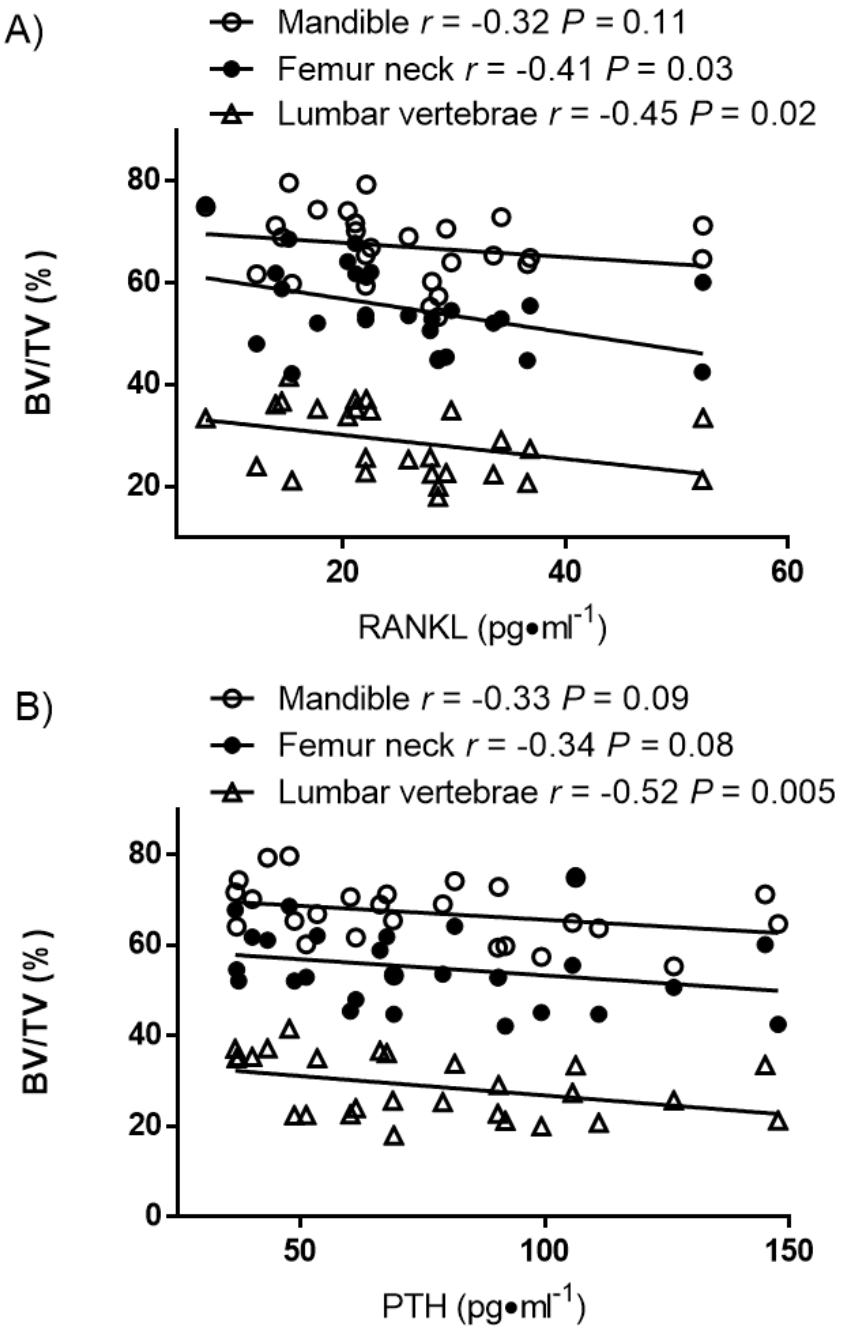

Figure 26: Correlation plots of RANKL and PTH with BV/TV at the mandible, femoral neck, and lumbar vertebrae
Correlation plots showing the data distributions for A) RANKL and B) PTH
n = 27-28 per site

CHAPTER 4: DISCUSSION

4.1 Main study findings:

Estrogen treatment attenuated the OVX-induced resorption of mandibular AB. The first objective of this research was to quantify the AB structure, density and strength following ERT. Estrogen treatment preserved the AB structure and density in the mandible of ovariectomized rats. The E2 treated group had, on average, a 9.8%, 12.0% and 11.5% higher BV/TV at the AB region, FN, and LB3 respectively compared to the OVX alone group. The density of an AB sub-region was also greater in the E2 treated group. The second objective was to investigate the relationship between AB following ERT and trabecular bone at the FN and LB3. The BV/TV of the AB region positively correlated with the BV/TV of the FN and LB3.

4.2 Mechanism of estrogen-mediated effects on AB:

In the maxillary AB of female rats treated with E2 (1.25 mg/kg), there was a reduction in osteoclast area, the number of nuclei per osteoclast, and the length of the osteoclast resorption surface with a higher number of smaller, mononucleated osteoclasts and smaller bone resorption surfaces [61]. E2 treatment effectively increased osteoclast apoptosis in the AB of the female rats [61]. Osteoclasts also exhibit a greater expression of estrogen receptor β in estrogen treated rats, suggesting a direct effect of the E2 on the osteoclasts located in the AB [62]. It is therefore likely that E2 reduces osteoclastic activity in the AB surrounding the first mandibular molar and, given that in our study design the serum E2 level was likely supraphysiological, it is probable that any increase in the rate of bone turnover caused by OVX in our estrogen treated rats was practically ablated. This proposed effect is supported by the

fact that our estrogen treated rat lumbar vertebral BV/TV was within a few percentage points of the lumbar vertebral BV/TV of sham treated rats from a different study [63].

4.3 Comparing our observed structural of both the alveolar bone of the mandible and the trabecular bone of the lumbar vertebral body to a single study that also investigated both sites but between sham and OVX groups:

The structure and density of both the AB of the mandible and the trabecular bone of the lumbar vertebral body was measured between sham and OVX groups at 12 weeks post-OVX [64]. Compared to our study design the rats used were older (6 months versus 3 months of age at OVX) and the lumbar vertebrae and mandible were scanned at a lower resolution (17 µm versus 9 µm). Both the lumbar vertebral body and mandibular AB ROI were similar to those used in our study, the lumbar vertebrae was based on the midpoint of the vertebral body and the AB was the entire interradicular septum of M1 ending at the mesial and distal root apices. By 12 weeks post-OVX there was a 17.6% difference in BV/TV at the lumbar vertebral body between the sham and OVX groups while our study found only a 11.5% difference in BV/TV between the E2 treated and OVX groups. However, by 12 weeks post-OVX no difference in mandibular AB BV/TV between the sham and OVX groups was reported despite a difference in SMI and trabecular pattern factor (Tb.Pf). With additional time post-OVX more deleterious changes to the AB occurred, by 24 weeks there was a difference in Tb.Th, connective density (Conn.D), and degree anisotropy and by 36 weeks a greater Tb.Sp. The small sample size used (n = 3 vs. n = 14) and the lower resolution µ-CT (17 µm vs. 9 µm) compared to our study likely contributed to the lack of a significant difference in BV/TV at the AB region between the sham and OVX groups. This theory is supported by the fact that there was a significant

difference in BMD in the same ROI reported at weeks 24 and 36 post-OVX with no significant difference in BV/TV at either of those times points. This study builds on the argument that AB, just like the trabecular bone of the lumbar vertebral body, is responsive to OVX and that changes to AB can be quantified with μ-CT.

4.4 DEXA and biomechanical strength testing are not specific enough to detect OVX-induced changes to alveolar bone:

Both DEXA and biomechanical strength testing were unable to reflect the changes in AB micro-architecture detected with μ-CT. The greater peak loads accepted by hemimandibles and femur midpoints of the OVX group were likely caused by longitudinal bone growth [65]. Such growth was likely disrupted in the E2 treated group, and was supported by the greater weight and height of the hemimandibles and LB3 respectively of the OVX group. Despite differences in growth, the parameters provided by μ-CT analysis showed significant differences in structure at the AB region, FN, and LB3. Although the AB region is not without its challenges even when assessed by μ-CT, examples include a relatively small ROI and high BV/TV compared to other sites, which are reflected in the fact that most of our SMI values are negative. SMI normally ranges from 0 to 3 representing a transition from plate-like to rod-like trabeculae within the ROI respectively [66]. A negative SMI is difficult to interpret but indicates very dense samples with concave plate-like trabeculae [67]. However, in the context of this study, it is the strong correlation among the sites in relation to the differences in their SMI that is the most important since it again emphasizes the sensitivity of AB to systemic skeletal changes.

The hemimandible and femur midpoints were stronger in the OVX group than the E2 treated group despite the femurs of the E2 treated rats having a greater areal

BMD. It is important to note that although the hemimandibles weighed more and the third lumbar vertebral bodies were taller from the OVX group compared to the E2 treated group, there were no differences in ROI size at any site used in the µ-CT analysis based on tissue volume (results not shown). Therefore the µ-CT results, unlike those from DEXA and biomechanical strength testing, are not biased by an increased bone size since there was no difference in ROI size between groups.

4.5 Effect of estrogen treatment in multiple skeletal sites after OVX:

To date, only one published study correlated mandibular AB with a site in the systemic skeleton; the proximal tibia [68]. As in our study, adult Sprague-Dawley rats were ovariectomized for 3 months and the mandibles and tibia were subjected to µ-CT and biomechanical strength testing. The estrogen treated rats received 10 µg/kg E2 by injection every other day for the 3 months post-OVX. The scan resolution was comparable to ours (10 µm vs. 9 µm) although the AB ROI differed from ours and extended from the incisor crest to the apices of the roots of M1 instead of just the interradicular septum of M1. In the study Tb.Th and Tb.Sp were correlated between the AB region and the proximal tibia; while in our study Tb.Th only correlated between the AB region and the LB3 but not the FN, and Tb.Sp correlated among the AB, FN and LB3. The study reported that the AB region BS/BV was correlated (r = 0.85) with the BS/BV of the proximal tibia and similarly in our study the AB region BV/TV was correlated at both the FN (r = 0.69) and LB3 (r = 0.75). Our study findings are thus in agreement and expand the literature by including sites clinically relevant for fracture. We observed our strongest correlations between the AB and LB3 at all parameters analyzed, and this is likely due to the reduced longitudinal

growth of the LB3 relative to a site such as the proximal tibia. Both this study and ours measured BMD with a μ-CT which is different from the areal BMD measured by DEXA. Areal BMD represents a two-dimensional picture of the mineral content, but not structure, of a bone ROI while BMD measured using μ-CT measures the density of a 3D structure within a ROI. In this study the higher BMD in the estrogen treated rats did not reach significance (1.24 vs. 1.32 $g \cdot cm^{-3}$) that is consistent with our findings (0.26 vs. 0.33 $g \cdot cm^{-3}$) keeping in mind that the differences in density are conserved despite the different ROI characteristics. Unlike our strength data, the estrogen treatment was trending on an improvement in peak load when testing the alveolar process below the molars instead of the midpoint of M1. Although the mandible micro-architecture was not directly compared between the sham, OVX, and E2 treated groups, the positive correlation with the proximal tibia and the fact that the tibia showed improvements in micro-architecture with E2 treatment support our findings that the AB of the mandible responds positively to estrogen treatment.

4.6 Characterization of the study estrogen dose:

The three most commonly used methods of estrogen administration in ovariectomized rat trials are: direct daily injection [69], subcutaneous slow release pellet placement [70], and estrogen taken orally in a matrix [71]. The best method is estrogen taken orally in a matrix (one example of a matrix is E2 in hazelnut cream spread) because it mimics the oral ERT taken by patients and results in serum levels of E2 that are both stable and within physiological limits [71]. In our study we used a slow-release pellet containing 1.5 mg of E2 to deliver approximately 17 μg of E2 per day for 90 days. The subcutaneous slow release pellet method was chosen because it

was designed to deliver a consistent daily estrogen dose without the time demands and stress on the animals of a daily injection. However, recent evidence suggests that the amount of estrogen released from the subcutaneous pellets is inconsistent over the duration claimed by the manufacturer [69-71]. We did notice a decrease in the food intake in the estrogen treated rats at week one and a lower body weight from weeks two through four without reduced food intake compared to the OVX group. It is likely that these changes in food intake and body weight are due to the estrogen intervention, since such changes were not observed in the OVX group that had a placebo pellet placed to account for the stress of the pellet placement surgery. It is logical that a reduced food intake would result in a reduced body weight, however, despite a reduction in food intake during week 1 alone following E2 pellet placement, there was a reduction in body weight between the E2 treated and OVX groups at weeks two, three and four of the study. Since there was no difference in food intake between the E2 treated and OVX groups during those weeks (weeks two through four), the difference in body weight is likely caused by the estrogen intervention. Additionally, because there is no difference in body weight past week four, it appears that whatever characteristic about the estrogen intervention that was causing the difference in body weight had ceased. This information indicates that the estrogen dose may not have been uniform across the treatment intervention and that a large amount of estrogen was released from the pellets at the beginning of the study. This inference is supported by a study that characterized the release of E2 from pellets identical to those used in this research, (1.5 mg, 90 slow release, from Innovative Research of America) and also in Sprague-Dawley rats that were of a similar age to

the ones used in our study (14 versus 12 weeks of age at OVX) [69]. Compared to a daily injection of 15 µg of E2, the serum concentrations in the pellet treated group were 73% higher at two weeks and 580% higher at four weeks than the injection group. A steady state in serum E2 was achieved two weeks earlier in the injection group compared to the pellet group.

In a follow-up study using a slow release pellet designed to give a daily dose of 4 µg for 60 days, much less than our 17 µg dose, it was found that the serum E2 concentration was highest two days after pellet placement and decreased over a 42 day observation period, but never to physiological E2 levels observed in intact rats. [70]. Even a much smaller dose slow release pellet designed to give a daily dose of 1 µg E2 for 90 days peaked at a concentration above the 4 µg per day pellet at two days after placement (528.0±51.5 pg/mL vs. 304.9±34.6 pg/mL; not statistically compared) and steadily declined until from days 35 to 42 the concentration was not significantly greater than ovariectomized controls. The injection group of 10 µg/kg E2 did not yield concentrations that were higher than the physiological range of rats euthanized during the normal estrus cycle (5.9–63.1 pg/mL) for the duration of the experiment [70].

In an experiment investigating the short-term effects of exogenous E2 administration (ranging from 30 minutes to seven days following treatment), the injection group (10 µg/kg) achieved physiological levels within four hours while the 1 µg per day pellet had an initial concentration ~ 30 times the physiological range and took seven days to achieve physiological levels. The 4 µg per day pellet never achieved serum levels within the physiological range even after seven days [71].

Although ERT or HRT in patients may commonly result in levels of serum estrogen higher than physiological levels, it should be noted that the aim of this study is not to recommend ERT or HRT as a strategy for tooth retention. It is unrealistic to extrapolate the dose of E2 used in this study to a current form of ERT or HRT given differences in the different mode of delivery (subcutaneous pellet vs. oral administration/transdermal patch) and potential inconsistent release of drug from the pellet. The purpose of this study is to highlight the responsiveness of AB to a known bone sparing agent, E2, and provide a rationale for using the ovx rat for developing dietary strategies that preserve bone at multiple skeletal sites, including the mandible.

Since our study used a slow release pellet which was designed to give a daily dose that was approximately four times greater (17 µg vs. 4 µg) than the 0.25 mg, 60 day slow release pellet previously described [71], it is likely that our estrogen treated rats experienced a spike in E2 concentration immediately following pellet placement and may only have achieved physiological levels near the end of the experiment. Just as in our study, when Sprague-Dawley rats were injected with 10 µg/kg E2 for 35 days they also experienced a reduced body weight and a reduction in longitudinal bone growth [65]. Since the estrogen dose used in our study was even higher - designed to release approximately 50 µg/kg E2 per day - and given the potential for an even higher daily dose than planned in the beginning of the study based on the characterized performance of the slow release pellets, it is likely that the reduced body weight observed in the estrogen treated rats and also the reduction in bone size (longitudinal bone growth) was caused by a high estrogen exposure.

4.7 Strengths and Limitations:

4.7.1 Strengths:

1. Large sample size: As seen in Tables 1-3, it is common for studies to use sample sizes less than 10 per group and even less than five per group. Our relatively large sample size substantiates our findings. For example, the change in BV/TV following ERT was a key determinant of AB preservation and based on our sample size of $n = 14$ the study was powered well over 99% to detect the observed difference between the means.
2. Standardized rodent diet: We chose a rodent diet that has been specifically developed to meet the nutritional requirements of mature rats [57] and thus have controlled for the influence of diet on the OVX-induced changes to AB. The relationship between mandibular density and dietary Ca (Section 1.3) highlights the importance of using a consistent diet in future studies. Future researchers can adopt AIN93M when attempting to reproduce the relationship between OVX and AB loss expressed in this work.
3. Multiple measurement techniques: We have used state-of-the-art μ-CT to precisely quantify changes to bone micro-architecture. Additionally we have investigated the relationship shown by μ-CT with more traditional measurements of total mineral content by DEXA and peak load until fracture by biomechanical strength testing. Plasma measures of bone remodeling were also assessed by multiplexing so that the localized changes to bone micro-architecture could be placed in the context of the systemic skeleton.

4. Correlations with bone turnover markers highlight preclinical model validity: In the clinical setting an increase in PTH has been associated with an increase in fracture incidence [72] which is in line with sustained levels of PTH stimulating bone turnover and resulting in bone catabolism [73]. Increased RANKL has not associated with fracture incidence [74] but an increase in RANKL is an indicator of increased osteoclastogenesis [75]. In our preclinical model the negative correlation between BV/TV at LB3 and plasma PTH levels supported the clinical increase in fracture risk. In terms of RANKL the BV/TV of both the LB3 and FN negatively correlated with the plasma RANKL levels, highlighting the expected inverse relationship between bone micro-architecture and osteoclastogenesis.

4.7.2 Limitations:

1. Lack of sham group: A limitation to our study design was the lack of a sham animal group which would both: account for any continued longitudinal bone growth that may be masking the effects of the OVX, and assess the efficacy of the estrogen intervention compared to an intact rat. An intact rat would facilitate the direct comparison between the effects of endogenous vs. exogenous estrogen on mandibular AB and provide a benchmark to compare the effects of the estrogen treatment in the context of physiological estrogen levels. A recent study with a similar design to ours contained only sham and OVX groups and assessed bone loss at multiple sites [63]. The rats were ovariectomized at 12 weeks of age as in our study and changes in trabecular micro-architecture were assessed at multiple skeletal sites including the third

and fourth lumbar vertebral bodies; this is an important site because it can be directly compared to changes we observed at L3. The µ-CT unit and scanning parameters were also very similar; they used a Skyscan 1072 at a 19 µm resolution while our study used a Skyscan 1176 at a 9 µm resolution. By 15 weeks post-OVX there was a significant difference in BV/TV between the sham (32.33 ± 4.14 %) and OVX (21.97 ± 1.03 %) groups. This is similar to the difference in BV/TV observed at 12 weeks post-OVX in our study between the E2 treated (34.66 ± 3.81 %) and OVX groups (23.19 ± 3.11%). Since our study did not include a sham group to compare the efficacy of the E2 treatment, this study is important because it suggests that our E2 treatment preserved the trabecular micro-architecture at the lumbar vertebral bodies to sham values; the BV/TV in our study of E2 treated rats was 34.66 % which is very close to the 32.33 % reported for the sham rats.

2. Characteristics specific of the ovariectomized rat model to consider when studying changes in AB: A limitation to the rat model for studying AB turnover is the fact that rat molars migrate distally throughout the lifespan [76]. This means that bone modeling occurs predominately on the mesial surfaces of the tooth while constant remodeling occurs on the distal surfaces [77]. Human teeth also migrate throughout life, but typically in the mesial direction [78]. OVX has been shown in the rat to accelerate AB turnover [79].
3. Inconsistent delivery of E2 from subcutaneous pellet: A limitation of the study was the potential for a spike in plasma E2 levels experienced by the rats when the pellets were first placed. Current research [71] into novel matrices to

administer E2 orally hold promise, but again this technique does not mimic all types of ERT available such as the transdermal patch..

CHAPTER 5: CONCLUSIONS

1) ERT preserved both the structure and density of the AB as determined by μ-CT in the preclinical model of postmenopausal osteoporosis.

2) The AB structure and density following ERT were correlated with the structure and density of trabecular bone at the FN and LB3.

5.1 Implications:

Estrogen treatment preserved the structure and density of mandibular AB in the preclinical rat model of postmenopausal osteoporosis. Differences in AB were mirrored by differences at the FN and LB3, which represent well-characterized sites of postmenopausal bone loss and subsequent fragility fracture. These correlations make a strong argument that an intervention – such as a drug or diet or supplement – to improve bone structure and density targeting these key sites of fracture may have beneficial effects on AB and thus tooth retention. Increased tooth retention is linked with better nutritional status [14, 16, 18, 19] and a healthful diet that supports overall skeletal health while reducing the risk of chronic disease [28]. Tooth loss and osteoporosis both occur with aging and thus clinical interventions aimed at bone preservation will benefit AB [80]. The mandible is not isolated from the rest of the skeleton, and to date AB turnover in the ovariectomized rat has been reduced by bisphosphonate (alendronate [30] and risedronate [31]) treatment, and AB formation has been stimulated by calcitonin [31] and intermittent PTH treatment [81]. Based on the capacity of the AB to characteristically respond to estrogen therapy in the context of well-characterized sites of postmenopausal bone loss, this preclinical model clearly

demonstrates its utility and importance in the development of future drug and nutritional interventions aimed at improving dental clinical practice with a special focus on tooth retention and thus the reduction of chronic disease.

CHAPTER 6: FUTURE DIRECTIONS

To strengthen the link between ERT and the preservation of AB in the ovariectomized rat model this study design could be replicated with the inclusion a sham group. This would help characterize the response of the AB to the ERT in the context of an unaltered control and account for any continued longitudinal bone growth.

Additionally, this proposed preclinical model of AB loss has centered around sex hormone deficiency in women and in the future should be expanded to include sex hormone deficient men represented with the orchidectomized rat model. To fully eliminate the competing influences of continued skeletal growth in the adult rat model, an aged rat (approximately six months) would ideally be used. Both of these critiques of the animal model bring the real purpose of the use of animal models into focus; the model is to best represent the human population that will directly benefit from the study intervention. Tooth loss is an age related phenomenon and the patients seeking restorative dental work are likely aged and thus in a state of sex hormone deficiency. By including orchidectomized rats into study designs and using a more aged model future studies can best represent the characteristics of the population likely to be encountered in clinical practice.

Since the aim of this preclinical model is to accurately represent changes to AB in an aged, sex hormone deficient clinical population it can be readily applied to

research involving implant placement and guided tissue regeneration. Estrogen deficiency has been shown to have systemic deleterious effects on the skeleton in this model, but it is important to keep in mind that the oral microenvironment is highly specialized [78] and therefore presents unique challenges to future drug or nutritional interventions. Understanding how factors such as the chronic inflammation characteristic of periodontal disease and other comorbidities interact is key to optimizing systemic skeletal therapy for the targeting of AB. The integration of AB preservation into existing systemic skeletal therapy is likely difficult, but the preclinical animal model presented in this work represents an attempt to bridge the gap, since there is clearly a relationship between the health of AB and the trabecular bone of the long bones and spine.

Nutrition is a modifiable lifestyle risk factor that represents a convergence among systemic bone health, AB health, tooth loss, and the risk of chronic disease. Clearly future preclinical studies aimed at improving AB health must use a multifaceted approach that considers both systemic skeletal health as well as individual lifestyle factors such as nutrition. Only then can inferences relevant to clinical practice be developed into effective strategies targeting an improved quality of life and reduce the risk of chronic disease.

References

1. Vaananen, H.K. and Harkonen, P.L., *Estrogen and bone metabolism.* Maturitas, 1996. **23 Suppl**: p. S65-69.
2. Pacifici, R., *Estrogen, cytokines, and pathogenesis of postmenopausal osteoporosis.* J Bone Miner Res, 1996. **11**(8): p. 1043-51.
3. Johnell, O. and Kanis, J.A., *An estimate of the worldwide prevalence and disability associated with osteoporotic fractures.* Osteoporos Int, 2006. **17**(12): p. 1726-33.
4. Oden, A., McCloskey, E.V., Johansson, H., and Kanis, J.A., *Assessing the impact of osteoporosis on the burden of hip fractures.* Calcif Tissue Int, 2013. **92**(1): p. 42-9.
5. Wright, N.C., Looker, A.C., Saag, K.G., Curtis, J.R., Delzell, E.S., Randall, S., and Dawson-Hughes, B., *The Recent Prevalence of Osteoporosis and Low Bone Mass in the United States Based on BMD at the FN or Lumbar Spine.* J Bone Miner Res, 2014.
6. Hopkins, R.B., Pullenayegum, E., Goeree, R., Adachi, J.D., Papaioannou, A., Leslie, W.D., Tarride, J.E., and Thabane, L., *Estimation of the lifetime risk of hip fracture for women and men in Canada.* Osteoporos Int, 2012. **23**(3): p. 921-7.
7. Tarride, J.E., Hopkins, R.B., Leslie, W.D., Morin, S., Adachi, J.D., Papaioannou, A., Bessette, L., Brown, J.P., and Goeree, R., *The burden of illness of osteoporosis in Canada.* Osteoporos Int, 2012. **23**(11): p. 2591-600.
8. Riggs, B.L., Khosla, S., and Melton, L.J., 3rd, *A unitary model for involutional osteoporosis: estrogen deficiency causes both type I and type II osteoporosis in postmenopausal women and contributes to bone loss in aging men.* J Bone Miner Res, 1998. **13**(5): p. 763-73.
9. Cauley, J.A., Wampler, N.S., Barnhart, J.M., Wu, L., Allison, M., Chen, Z., Hendrix, S., Robbins, J., Jackson, R.D., and Women's Health Initiative Observational, S., *Incidence of fractures compared to cardiovascular disease and breast cancer: the Women's Health Initiative Observational Study.* Osteoporos Int, 2008. **19**(12): p. 1717-23.
10. Johnell, O. and Kanis, J., *Epidemiology of osteoporotic fractures.* Osteoporos Int, 2005. **16 Suppl 2**: p. S3-7.
11. Johnell, O., Kanis, J.A., Oden, A., Sernbo, I., Redlund-Johnell, I., Petterson, C., De Laet, C., and Jonsson, B., *Mortality after osteoporotic fractures.* Osteoporos Int, 2004. **15**(1): p. 38-42.
12. Darcey, J., Horner, K., Walsh, T., Southern, H., Marjanovic, E.J., and Devlin, H., *Tooth loss and osteoporosis: to assess the association between osteoporosis status and tooth number.* British Dental Journal, 2013. **214**(4): p. 1-10.
13. Iwasaki, M., Nakamura, K., Yoshihara, A., and Miyazaki, H., *Change in BMD and tooth loss in Japanese community-dwelling postmenopausal women: a 5-year cohort study.* J Bone Miner Metab, 2012. **30**(4): p. 447-53.
14. Krall, E.A., Garcia, R.I., and Dawson-Hughes, B., *Increased risk of tooth loss is related to bone loss at the whole body, hip, and spine.* Calcif Tissue Int, 1996. **59**(6): p. 433-7.
15. Payne, J.B., Reinhardt, R.A., Nummikoski, P.V., and Patil, K.D., *Longitudinal AB loss in postmenopausal osteoporotic/osteopenic women.* Osteoporos Int, 1999. **10**(1): p. 34-40.
16. Sheiham, A., Steele, J.G., Marcenes, W., Lowe, C., Finch, S., Bates, C.J., Prentice, A., and Walls, A.W., *The relationship among dental status, nutrient intake, and nutritional status in older people.* J Dent Res, 2001. **80**(2): p. 408-13.

17. Ervin, R.B. and Dye, B.A., *The effect of functional dentition on Healthy Eating Index scores and nutrient intakes in a nationally representative sample of older adults.* J Public Health Dent, 2009. **69**(4): p. 207-16.
18. Sahyoun, N.R., Lin, C.L., and Krall, E., *Nutritional status of the older adult is associated with dentition status.* J Am Diet Assoc, 2003. **103**(1): p. 61-6.
19. Brennan, D.S., Singh, K.A., Liu, P., and Spencer, A., *Fruit and vegetable consumption among older adults by tooth loss and socio-economic status.* Aust Dent J, 2010. **55**(2): p. 143-9.
20. Cauley, J.A., Robbins, J., Chen, Z., Cummings, S.R., Jackson, R.D., LaCroix, A.Z., LeBoff, M., Lewis, C.E., McGowan, J., Neuner, J., Pettinger, M., Stefanick, M.L., Wactawski-Wende, J., Watts, N.B., and Women's Health Initiative, I., *Effects of estrogen plus progestin on risk of fracture and BMD: the Women's Health Initiative randomized trial.* JAMA, 2003. **290**(13): p. 1729-38.
21. Jackson, R.D., Wactawski-Wende, J., LaCroix, A.Z., Pettinger, M., Yood, R.A., Watts, N.B., Robbins, J.A., Lewis, C.E., Beresford, S.A., Ko, M.G., Naughton, M.J., Satterfield, S., Bassford, T., and Women's Health Initiative, I., *Effects of conjugated equine estrogen on risk of fractures and BMD in postmenopausal women with hysterectomy: results from the women's health initiative randomized trial.* J Bone Miner Res, 2006. **21**(6): p. 817-28.
22. Grodstein, F., Colditz, G.A., and Stampfer, M.J., *Post-menopausal hormone use and tooth loss: a prospective study.* J Am Dent Assoc, 1996. **127**(3): p. 370-7.
23. Paganini-Hill, A., *The benefits of estrogen replacement therapy on oral health. The Leisure World cohort.* Arch Intern Med, 1995. **155**(21): p. 2325-9.
24. Krall, E.A., DawsonHughes, B., Hannan, M.T., Wilson, P.W.F., and Kiel, D.P., *Postmenopausal estrogen replacement and tooth retention.* American Journal of Medicine, 1997. **102**(6): p. 536-542.
25. Taguchi, A., Sanada, M., Suei, Y., Ohtsuka, M., Nakamoto, T., Lee, K., Tsuda, M., Ohama, K., Tanimoto, K., and Bollen, A.M., *Effect of estrogen use on tooth retention, oral bone height, and oral bone porosity in Japanese postmenopausal women.* Menopause, 2004. **11**(5): p. 556-62.
26. Civitelli, R., Pilgram, T.K., Dotson, M., Muckerman, J., Lewandowski, N., Armamento-Villareal, R., Yokoyama-Crothers, N., Kardaris, E.E., Hauser, J., Cohen, S., and Hildebolt, C.F., *Alveolar and postcranial bone density in postmenopausal women receiving hormone/estrogen replacement therapy: a randomized, double-blind, placebo-controlled trial.* Arch Intern Med, 2002. **162**(12): p. 1409-15.
27. Ross, A.C., Manson, J.E., Abrams, S.A., Aloia, J.F., Brannon, P.M., Clinton, S.K., Durazo-Arvizu, R.A., Gallagher, J.C., Gallo, R.L., Jones, G., Kovacs, C.S., Mayne, S.T., Rosen, C.J., and Shapses, S.A., *The 2011 report on dietary reference intakes for calcium and vitamin D from the Institute of Medicine: what clinicians need to know.* J Clin Endocrinol Metab, 2011. **96**(1): p. 53-8.
28. Boeing, H., Bechthold, A., Bub, A., Ellinger, S., Haller, D., Kroke, A., Leschik-Bonnet, E., Muller, M.J., Oberritter, H., Schulze, M., Stehle, P., and Watzl, B., *Critical review: vegetables and fruit in the prevention of chronic diseases.* Eur J Nutr, 2012. **51**(6): p. 637-63.

29. Chen, Y.M., Ho, S.C., and Woo, J.L., *Greater fruit and vegetable intake is associated with increased bone mass among postmenopausal Chinese women.* Br J Nutr, 2006. **96**(4): p. 745-51.
30. Duarte, P.M., Goncalves, P., Casati, M.Z., de Toledo, S., Sallum, E.A., and Nociti, F.H., Jr., *Estrogen and alendronate therapies may prevent the influence of estrogen deficiency on the tooth-supporting AB: a histometric study in rats.* J Periodontal Res, 2006. **41**(6): p. 541-6.
31. Hunziker, J., Wronski, T.J., and Miller, S.C., *Mandibular bone formation rates in aged ovariectomized rats treated with anti-resorptive agents alone and in combination with intermittent parathyroid hormone.* J Dent Res, 2000. **79**(6): p. 1431-8.
32. Thompson, D.D., Simmons, H.A., Pirie, C.M., and Ke, H.Z., *FDA Guidelines and animal models for osteoporosis.* Bone, 1995. **17**(4 Suppl): p. 125S-133S.
33. Turner, C.H., Roeder, R.K., Wieczorek, A., Foroud, T., Liu, G., and Peacock, M., *Variability in skeletal mass, structure, and biomechanical properties among inbred strains of rats.* J Bone Miner Res, 2001. **16**(8): p. 1532-9.
34. Sengupta, S., Arshad, M., Sharma, S., Dubey, M., and Singh, M.M., *Attainment of peak bone mass and bone turnover rate in relation to estrous cycle, pregnancy and lactation in colony-bred Sprague-Dawley rats: suitability for studies on pathophysiology of bone and therapeutic measures for its management.* J Steroid Biochem Mol Biol, 2005. **94**(5): p. 421-9.
35. Lelovas, P.P., Xanthos, T.T., Thoma, S.E., Lyritis, G.P., and Dontas, I.A., *The laboratory rat as an animal model for osteoporosis research.* Comp Med, 2008. **58**(5): p. 424-30.
36. Leitner, M.M., Tami, A.E., Montavon, P.M., and Ito, K., *Longitudinal as well as age-matched assessments of bone changes in the mature ovariectomized rat model.* Lab Anim, 2009. **43**(3): p. 266-71.
37. Jee, W.S. and Yao, W., *Overview: animal models of osteopenia and osteoporosis.* J Musculoskelet Neuronal Interact, 2001. **1**(3): p. 193-207.
38. Kalu, D.N., *The ovariectomized rat model of postmenopausal bone loss.* Bone Miner, 1991. **15**(3): p. 175-91.
39. Wronski, T.J., Cintron, M., and Dann, L.M., *Temporal relationship between bone loss and increased bone turnover in ovariectomized rats.* Calcif Tissue Int, 1988. **43**(3): p. 179-83.
40. Li, M., Shen, Y., and Wronski, T.J., *Time course of FN osteopenia in ovariectomized rats.* Bone, 1997. **20**(1): p. 55-61.
41. Wronski, T.J., Dann, L.M., and Horner, S.L., *Time course of vertebral osteopenia in ovariectomized rats.* Bone, 1989. **10**(4): p. 295-301.
42. Tanaka, M., Ejiri, S., Toyooka, E., Kohno, S., and Ozawa, H., *Effects of OVX on trabecular structures of rat AB.* J Periodontal Res, 2002. **37**(2): p. 161-5.
43. Irie, K., Sakakura, Y., Tsuruga, E., Hosokawa, Y., and Yajima, T., *Three-dimensional changes of the mandible and AB in the ovariectomized rat examined by micro-focus computed tomography.* J Jpn Soc Periodontal, 2004. **46**(4): p. 288-293.
44. Ames, M.S., Hong, S., Lee, H.R., Fields, H.W., Johnston, W.M., and Kim, D.G., *Estrogen deficiency increases variability of tissue mineral density of AB surrounding teeth.* Arch Oral Biol, 2010. **55**(8): p. 599-605.
45. Moriya, Y., Ito, K., and Murai, S., *Effects of experimental osteoporosis on AB loss in rats.* J Oral Sci, 1998. **40**(4): p. 171-5.

46. Elovic, R.P., Hipp, J.A., and Hayes, W.C., *Maxillary molar extraction decreases stiffness of the mandible in ovariectomized rats.* J Dent Res, 1994. **73**(11): p. 1735-41.
47. Patullo, I.M., Takayama, L., Patullo, R.F., Jorgetti, V., and Pereira, R.M., *Influence of OVX and masticatory hypofunction on mandibular bone remodeling.* Oral Dis, 2009. **15**(8): p. 580-6.
48. Hara, T., Sato, T., Oka, M., Mori, S., and Shirai, H., *Effects of OVX and/or dietary calcium deficiency on bone dynamics in the rat hard palate, mandible and proximal tibia.* Arch Oral Biol, 2001. **46**(5): p. 443-51.
49. Yang, J., Pham, S.M., and Crabbe, D.L., *Effects of oestrogen deficiency on rat mandibular and tibial microarchitecture.* Dentomaxillofac Radiol, 2003. **32**(4): p. 247-51.
50. Mavropoulos, A., Rizzoli, R., and Ammann, P., *Different responsiveness of alveolar and tibial bone to bone loss stimuli.* J Bone Miner Res, 2007. **22**(3): p. 403-10.
51. Elovic, R.P., Hipp, J.A., and Hayes, W.C., *OVX decreases the bone area fraction of the rat mandible.* Calcif Tissue Int, 1995. **56**(4): p. 305-10.
52. Tanaka, M., Toyooka, E., Kohno, S., Ozawa, H., and Ejiri, S., *Long-term changes in trabecular structure of aged rat AB after OVX.* Oral Surg Oral Med Oral Pathol Oral Radiol Endod, 2003. **95**(4): p. 495-502.
53. Jiang, G., Matsumoto, H., and Fujii, A., *Mandible bone loss in osteoporosis rats.* J Bone Miner Metab, 2003. **21**(6): p. 388-95.
54. Jiang, G.Z., Matsumoto, H., Hori, M., Gunji, A., Hakozaki, K., Akimoto, Y., and Fujii, A., *Correlation among geometric, densitometric, and mechanical properties in mandible and femur of osteoporotic rats.* J Bone Miner Metab, 2008. **26**(2): p. 130-137.
55. Kuroda, S., Mukohyama, H., Kondo, H., Aoki, K., Ohya, K., Ohyama, T., and Kasugai, S., *BMD of the mandible in ovariectomized rats: analyses using dual energy X-ray absorptiometry and peripheral quantitative computed tomography.* Oral Dis, 2003. **9**(1): p. 24-8.
56. Yang, J., Farnell, D., Devlin, H., Horner, K., and Graham, J., *The effect of OVX on mandibular cortical thickness in the rat.* J Dent, 2005. **33**(2): p. 123-9.
57. Reeves, P.G., Nielsen, F.H., and Fahey, G.C., Jr., *AIN-93 purified diets for laboratory rodents: final report of the American Institute of Nutrition ad hoc writing committee on the reformulation of the AIN-76A rodent diet.* J Nutr, 1993. **123**(11): p. 1939-51.
58. Kawamoto, S., Ejiri, S., Nagaoka, E., and Ozawa, H., *Effects of oestrogen deficiency on osteoclastogenesis in the rat periodontium.* Arch Oral Biol, 2002. **47**(1): p. 67-73.
59. Hidaka, S., Okamoto, Y., Yamada, Y., Miyazaki, K., and Kimura, T., *Alterations in the periodontium after OVX in rats: the effects of a Japanese herbal medicine, Chujo-to.* Phytother Res, 2000. **14**(7): p. 527-33.
60. Jiang, G., Matsumoto, H., Yamane, J., Kuboyama, N., Akimoto, Y., and Fujii, A., *Prevention of trabecular bone loss in the mandible of ovariectomized rats.* J Oral Sci, 2004. **46**(2): p. 75-85.
61. Faloni, A.P., Sasso-Cerri, E., Rocha, F.R., Katchburian, E., and Cerri, P.S., *Structural and functional changes in the AB osteoclasts of estrogen-treated rats.* J Anat, 2012. **220**(1): p. 77-85.
62. Crusode de Souza, M., Sasso-Cerri, E., and Cerri, P.S., *Immunohistochemical detection of estrogen receptor beta in AB cells of estradiol-treated female rats: possible direct action of estrogen on osteoclast life span.* J Anat, 2009. **215**(6): p. 673-81.

63. Francisco, J.I., Yu, Y., Oliver, R.A., and Walsh, W.R., *Relationship between age, skeletal site, and time post-OVX on bone mineral and trabecular microarchitecture in rats.* J Orthop Res, 2011. **29**(2): p. 189-96.
64. Liu, X.L., Li, C.L., Lu, W.W., Cai, W.X., and Zheng, L.W., *Skeletal site-specific response to OVX in a rat model: change in bone density and microarchitecture.* Clin Oral Implants Res, 2014.
65. Wronski, T.J., Cintron, M., Doherty, A.L., and Dann, L.M., *Estrogen treatment prevents osteopenia and depresses bone turnover in ovariectomized rats.* Endocrinology, 1988. **123**(2): p. 681-6.
66. Bouxsein, M.L., Boyd, S.K., Christiansen, B.A., Guldberg, R.E., Jepsen, K.J., and Muller, R., *Guidelines for assessment of bone microstructure in rodents using micro-computed tomography.* J Bone Miner Res, 2010. **25**(7): p. 1468-86.
67. Hildebrand, T., Laib, A., Muller, R., Dequeker, J., and Ruegsegger, P., *Direct three-dimensional morphometric analysis of human cancellous bone: microstructural data from spine, femur, iliac crest, and calcaneus.* J Bone Miner Res, 1999. **14**(7): p. 1167-74.
68. Liu, H., Gao, K., Lin, H., Zhang, Y., and Li, B., *Relative Skeletal Effects in Different Sites of the Mandible with the Proximal Tibia during OVX and the Subsequent Estrogen Treatment.* J Oral Implantol, 2014.
69. Theodorsson, A., Hilke, S., Rugarn, O., Linghammar, D., and Theodorsson, E., *Serum concentrations of 17beta-estradiol in ovariectomized rats during two times six weeks crossover treatment by daily injections in comparison with slow-release pellets.* Scand J Clin Lab Invest, 2005. **65**(8): p. 699-705.
70. Strom, J.O., Theodorsson, E., and Theodorsson, A., *Order of magnitude differences between methods for maintaining physiological 17beta-oestradiol concentrations in ovariectomized rats.* Scand J Clin Lab Invest, 2008. **68**(8): p. 814-22.
71. Isaksson, I.M., Theodorsson, A., Theodorsson, E., and Strom, J.O., *Methods for 17beta-oestradiol administration to rats.* Scand J Clin Lab Invest, 2011. **71**(7): p. 583-92.
72. Garnero, P., Sornay-Rendu, E., Claustrat, B., and Delmas, P.D., *Biochemical markers of bone turnover, endogenous hormones and the risk of fractures in postmenopausal women: the OFELY study.* J Bone Miner Res, 2000. **15**(8): p. 1526-36.
73. Poole, K.E. and Reeve, J., *Parathyroid hormone - a bone anabolic and catabolic agent.* Curr Opin Pharmacol, 2005. **5**(6): p. 612-7.
74. LaCroix, A.Z., Jackson, R.D., Aragaki, A., Kooperberg, C., Cauley, J.A., Chen, Z., Leboff, M.S., Duggan, D., and Wactawski-Wende, J., *OPG and sRANKL serum levels and incident hip fracture in postmenopausal Caucasian women in the Women's Health Initiative Observational Study.* Bone, 2013. **56**(2): p. 474-81.
75. Khosla, S., *Minireview: the OPG/RANKL/RANK system.* Endocrinology, 2001. **142**(12): p. 5050-5.
76. Vignery, A. and Baron, R., *Dynamic histomorphometry of AB remodeling in the adult rat.* Anat Rec, 1980. **196**(2): p. 191-200.
77. King, G.J., Latta, L., Rutenberg, J., Ossi, A., and Keeling, S.D., *AB turnover in male rats: site- and age-specific changes.* Anat Rec, 1995. **242**(3): p. 321-8.
78. Saffar, J.L., Lasfargues, J.J., and Cherruau, M., *AB and the alveolar process: the socket that is never stable.* Periodontol 2000, 1997. **13**: p. 76-90.

79. Yamashiro, T. and Takano-Yamamoto, T., *Influences of OVX on experimental tooth movement in the rat.* J Dent Res, 2001. **80**(9): p. 1858-61.
80. Seldin, E.B., *Is there any reason to suspect that the determinants of mandibular BMD might differ from those of systemic skeletal BMD?* Menopause, 2012. **19**(6): p. 608-9.
81. Miller, S.C., Hunziker, J., Mecham, M., and Wronski, T.J., *Intermittent parathyroid hormone administration stimulates bone formation in the mandibles of aged ovariectomized rats.* J Dent Res, 1997. **76**(8): p. 1471-6.